

Thermophysical properties of the liquid organic hydrogen carrier system based on benzyltoluene considering influences of isomerism and dissolved hydrogen

Manuel Kerscher^a, Julius H. Jander^a, Junwei Cui^{a,1}, Lukas A. Maurer^b, Patrick Wolf^{b,2}, Jonas D. Hofmann^b, Anil Köksal^a, Hannah Zachskorn^a, Franziska Auer^b, Peter S. Schulz^c, Peter Wasserscheid^{b,c,d}, Michael H. Rausch^a, Thomas M. Koller^{a,*}, Andreas P. Fröba^a

^a Institute of Advanced Optical Technologies – Thermophysical Properties (AOT-TP), Department of Chemical and Biological Engineering (CBI) and Erlangen Graduate School in Advanced Optical Technologies (SAOT), Friedrich-Alexander-Universität Erlangen-Nürnberg (FAU), Paul-Gordan-Straße 8, 91052 Erlangen, Germany

^b Forschungszentrum Jülich GmbH, Helmholtz Institute Erlangen-Nürnberg for Renewable Energy (IEK-11), Cauerstraße 1, 91058 Erlangen, Germany

^c Institute of Chemical Reaction Engineering (CRT), Department of Chemical and Biological Engineering (CBI), Friedrich-Alexander-Universität Erlangen-Nürnberg (FAU), Egerlandstraße 3, 91058 Erlangen, Germany

^d Forschungszentrum Jülich GmbH, Institute for a Sustainable Hydrogen Economy, Am Brainery Park 4, 52428 Jülich, Germany

ARTICLE INFO

Handling Editor: Prof. J. W. Sheffield

Keywords:

Benzyltoluene

Hydrogen

Liquid organic hydrogen carrier

Mixture behavior

Regioisomers

Thermophysical properties

ABSTRACT

The benzyltoluene (BT)-based liquid organic hydrogen carrier (LOHC) system currently considered for large-scale applications represents a mixture of regioisomers. To characterize this complex system, a comprehensive experimental database for various thermophysical properties of synthesized BT isomers and their mixtures without and with the presence of hydrogen (H₂) close to vapor-liquid equilibrium is established using optical and conventional techniques at process-relevant temperatures and pressures up to 573 K and 6 MPa. The surface tension varies by less than 4% among the dehydrogenated (H0-BT) or hydrogenated (H12-BT) isomers. The density and viscosity of mixtures of H0-BT or H12-BT isomers can be described by simple mixing rules with average absolute relative deviations of 0.022% and 0.38%. With increasing H₂ pressure, the viscosity remains nearly constant, while the interfacial tension decreases by up to 5%. The thermal and mutual diffusivity of H12-ortho-BT containing dissolved H₂ at 6 MPa decrease and increase with increasing temperature.

1. Introduction

For the efficient and economically viable use of green hydrogen (H₂) obtained by water electrolysis using electricity from renewable energy sources, a global infrastructure for its storage and transport needs to be established. Considering the volatile and flammable nature as well as the small volumetric energy density of gaseous H₂ at ambient conditions, a multitude of options for the efficient and safe storage of H₂ are discussed. In addition to the established approaches of compression or liquefaction [1,2], alternative ways of storage like physical adsorption

[3,4], in metal hydrides [5,6], or in other hydrides like methanol [7,8] and ammonia [9,10] have been considered. In the recent years, also liquid organic hydrogen carriers (LOHCs) have attained considerable interest for the storage and transport of H₂ at reasonable volumetric and gravimetric energy densities based on reversible cycles of catalytic hydrogenation and dehydrogenation reactions [11–13]. Here, the compatibility of hydrocarbon LOHCs in combination with the existing infrastructure for liquid fossil fuels [14,15] is highly relevant for a fast transition towards the usage of renewable energy sources around the globe.

Among different heteroaromatic [12,16,17] and purely

* Corresponding author.

E-mail addresses: manuel.kerscher@fau.de (M. Kerscher), julius.jander@fau.de (J.H. Jander), jwcui@chd.edu.cn (J. Cui), l.maurer@fz-juelich.de (L.A. Maurer), patrick.s.wolf@gmx.de (P. Wolf), jonas.d.hofmann@gmx.de (J.D. Hofmann), anil.koeksal@fau.de (A. Köksal), hannah.zachskorn@fau.de (H. Zachskorn), f.auer@fz-juelich.de (F. Auer), peter.schulz@fau.de (P.S. Schulz), peter.wasserscheid@fau.de (P. Wasserscheid), michael.rausch@fau.de (M.H. Rausch), thomas.m.koller@fau.de (T.M. Koller), andreas.p.froeba@fau.de (A.P. Fröba).

¹ Current address: School of Energy and Electrical Engineering, Chang'an University, 710064 Xi'an, China.

² Current address: Evonik Operations GmbH, Rodenbacher Chaussee 4, 63457 Hanau, Germany.

Abbreviations			
AARD	average absolute relative deviation	H0-DPM or DPM	diphenylmethane
CF	correlation function	H6-DPM	cyclohexylphenylmethane
CV	capillary viscometry	H12-DPM	dicyclohexylmethane
DLS	dynamic light scattering	LOHC	liquid organic hydrogen carrier
DoH	degree of hydrogenation	m	meta
GC-FID	gas chromatography with coupled flame-ionization detection	NMR	nuclear magnetic resonance
H0-BT or BT	benzyltoluene	o	ortho
H6-BT	cyclohexylmethyl-methylbenzene	p	para
H12-BT	perhydrobenzyltoluene	PD	pendant drop
H0-DBT	dibenzyltoluene	SDBS	Spectral Database for Organic Compounds
H18-DBT	perhydrodibenzyltoluene	SLS	surface light scattering
		VTD	vibrating-tube densimetry
		YL	Young-Laplace

hydrocarbon-based cyclic [18–21] LOHC systems discussed in the literature, the system based on benzyltoluene (BT) is currently considered as one of the most promising candidates. It is not only available in large amounts as heat transfer oil, but also shows relatively low melting and relatively high boiling points in combination with a considerable H₂ storage capacity of 6.2 wt-% [14,22,23]. In comparison to the structurally similar system based on dibenzyltoluene (DBT, H0-DBT), the distinctly lower viscosity and faster dehydrogenation kinetics demonstrated in recent studies [19,23,24] make the BT-based system more attractive for large-scale applications.

For the modeling of processes and the proper design of corresponding apparatuses, accurate data for the thermophysical properties at process-relevant conditions are required. This also applies to the properties density, surface tension, viscosity, thermal diffusivity, and Fick diffusivity which are in the focus of the present work. The latter three transport properties are key parameters for the description of the molecular transport of momentum, heat, and mass, respectively. The viscosity, for example, influences the pumpability of the fluid. The density is important for, e.g., the dimensioning of process units or storage vessels, while the interfacial tension affects wetting of the solid catalyst and the bubble formation during dehydrogenation. For all these thermophysical properties, corresponding experimental data are hardly available for the BT-based LOHC system to date, although they are necessary for its efficient large-scale industrial application. The fact that the commercially available BT-based heat carrier oil consists of three regioisomers of the dehydrogenated benzyltoluene (H0-BT) complicates the characterization of this LOHC with respect to its thermophysical properties. Recent studies have shown that its H₂ storage and release rates strongly depend on the regioisomeric composition [21,25]. This may also be expected for the thermophysical properties as it is known, for instance, that the liquid density ρ and liquid dynamic viscosity η of the regioisomers of xylene at a temperature T of 298.15 K vary by up to 2.2% and 30% [26]. Similar variations can also be anticipated for isomeric mixtures of BT, which influences the performance and design of the LOHC process.

The hydrogenation of H0-BT represents a multi-step reaction involving intermediate products in the form of various isomers of the partially hydrogenated BT (cyclohexylmethyl-methylbenzene, H6-BT) [25]. Considering that nine H6-BT isomers exist and each of the three regioisomer of the fully hydrogenated perhydrobenzyltoluene (H12-BT) features two stereoisomeric configurations, the complexity with respect to the characterization of the BT-based system further increases. At least with respect to the stereoisomers of H12-BT, Lamneck and Wise [27] could isolate the six isomers and found considerable differences in ρ and η between the stereoisomers of a given regioisomer of up to 1.4% and 34% measured at $T = (293 \text{ and } 311) \text{ K}$, respectively. Besides their work reporting data for ρ and η covering T up to 373 K for the latter property, only a few experimental studies on ρ , η , and the surface tension σ of BT

and its partially and fully hydrogenated isomers can be found in the literature. While for H0-meta-BT (H0-m-BT) [28] and H0-para-BT (H0-p-BT) [29–31], ρ data at T between (288 and 298) K have been reported, no further information could be found for η and σ of the dehydrogenated regioisomers. Considering η , σ , and ρ of the regio- and stereoisomers of H12-BT, data are only accessible from the work of Lamneck and Wise [27]. In the context of its application as an LOHC, Müller et al. [32] have studied η , σ , and ρ at T up to (453, 328, and 473) K, respectively, for the commercially available isomeric mixture of H0-BT with the trade name Marlotherm LH as well as a corresponding fully hydrogenated mixture obtained by catalytic hydrogenation of the H0-BT sample. In their work, the isomeric composition of H0-BT and H12-BT is not specified, which impedes an interpretation of the mixing behavior of the isomers. All data summarized so far have been obtained for pressures p of about 0.1 MPa. Regarding the influence of dissolved H₂ being present especially during hydrogenation reactions at elevated p , experimental studies for η and σ are only available for the structurally similar LOHC system based on diphenylmethane (DPM, H0-DPM) [33, 34], which serve for comparison purposes in the present work. As this system does not exhibit regioisomerism owing to the absence of methyl groups bonded to the carbon rings, its characterization with respect to thermophysical properties is considerably simpler. Thus, the DPM-based system can be regarded as a reference system. Furthermore, no information on Fick diffusion coefficients D_{11} influencing the reaction kinetics during hydrogenation and dehydrogenation can be found for mixtures of the BT-based systems with dissolved H₂. In summary, there is currently a clear lack of accurate data for the mentioned thermophysical properties of the BT-based isomers and their mixtures, especially at process-relevant conditions covering T up to about 600 K and p up to about 5 MPa in the presence of H₂ [23,36,37].

The present work comprises a comprehensive experimental study on η , σ , and ρ of the regioisomers of H0-BT and H12-BT including corresponding mixtures at $p \approx 0.1 \text{ MPa}$ and T up to (573, 573, and 473) K, respectively. For this, the six regioisomers of H0-BT and H12-BT were synthesized with high purities, where the obtained stereoisomeric composition of the H12-BT regioisomers was characterized. For the measurement of the thermophysical properties, the same conventional and light scattering methods were applied which have been successfully used for corresponding research on the DPM-based system [33–35]. The pure regioisomers as well as H0- and H12-BT-based mixtures with the same degree of hydrogenation (DoH) were studied by capillary viscometry (CV) for η , the pendant-drop (PD) method for σ , surface light scattering (SLS) for the simultaneous determination of η and σ , and vibrating-tube densimetry (VTD) for ρ . In order to approach the DoH-dependent behavior of realistic, H6-BT-containing LOHC mixtures during hydrogenation and dehydrogenation reactions, mixtures of H0-ortho-BT (H0-o-BT) and H12-ortho-BT (H12-o-BT) were additionally investigated as simplified but well-defined model systems by CV,

PD, and VTD. Here, the ortho-regioisomers were chosen due to their technical relevance in view of their relatively large share in the technical mixtures currently used as LOHC system. Based on the experimental data, mixing rules and estimation schemes were tested to identify appropriate calculation tools for the thermophysical properties of interest at varying isomeric composition or *DoH*. Furthermore, several thermophysical properties under the influence of dissolved H₂ were studied exemplarily for H12-o-BT. The impact of pressurized H₂ on η and σ was probed using the PD method and SLS for *p* up to 6 MPa and *T* between (323 and 523) K. Dynamic light scattering (DLS) measurements in the bulk of the saturated liquid phase in the same *T* range additionally gave access to the Fick diffusion coefficient *D*₁₁ and the thermal diffusivity *a* of binary mixtures of H12-o-BT and dissolved H₂ at *p* = 6 MPa.

2. Experimental section

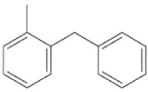
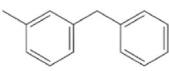
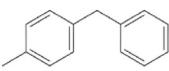
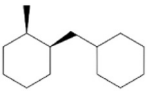
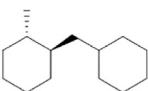
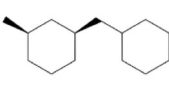
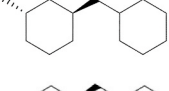
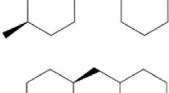
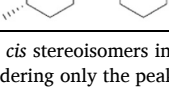
2.1. Materials and sample preparation

The regioisomers of H0-BT and H12-BT were synthesized using corresponding commercially available regioisomers of methylbenzophenone as a starting material. Details on the synthesis procedure involving an initial catalytic hydrodeoxygenation step followed by a catalytic hydrogenation reaction to obtain the H12-BT regioisomers or a catalytic dehydrogenation reaction for the purification of H0-BT regioisomers are given in section S1 of the Supporting Information. The six samples of pure regioisomers were analyzed by gas chromatography equipped with a flame-ionization detector (GC-FID). Since the H12-BT regioisomers represent mixtures of their *cis* and *trans* stereoisomers, where the composition is influenced by the reaction kinetics during hydrogenation, their distribution was also quantified. For an initial assignment of the related GC peaks, the three H12-BT regioisomer samples were additionally analyzed by carbon-13 nuclear magnetic resonance (¹³C NMR) spectroscopy. The *cis* and *trans* isomers were distinguished using the different values of the chemical shifts of the respective methyl group. The assignment of the measured values of the six isomers was realized based on spectra for the isomers of dimethylcyclohexane obtained from the Spectral Database for Organic Compounds (SDBS) [38]. By using the inverse gate ¹³C pulse sequence, the signals could be evaluated quantitatively. For each regioisomer, the clearly different amounts of the *cis* and *trans* conformers identified by ¹³C NMR allowed to assign the corresponding GC peaks based on the comparison of signal intensity ratios in NMR and GC, where the latter analysis was considered for the final quantification of the stereoisomeric distribution. Further information on the GC analysis of the synthesized regioisomers is included in section S2 of the Supporting Information. In Table 1, the mole fractions of the *cis* stereoisomers *x*_{cis} in the H12-BT regioisomers are included, where the mole fractions of the *trans* stereoisomers can be derived by *x*_{trans} = 1 – *x*_{cis}, i.e., impurities in the sample are not considered. The purities of all six regioisomer samples determined by GC-FID are given in Table 1 in terms of peak area fractions. Here, all GC peaks after elution of the solvent peak that cannot be assigned to the respective regioisomers are regarded as impurities and may also include other regioisomers. The impurities are found to be mostly partially hydrogenated H6-BT isomers or high boilers including methylfluorene and anthracene as well as related derivatives.

In addition to the pure regioisomers, the commercially available isomeric mixture of H0-BT with the trade name Marlotherm LH (in the following H0-BT) was purchased from Eastman Chemical Company. A catalytic hydrogenation of H0-BT was performed according to the routine described in section S1 of the Supporting Information to obtain a sample of H12-BT with a regioisomeric composition similar to that of the educt. Corresponding information is disclosed in Table 2 together with the impurities based on peak areas measured by GC-FID, where any GC peak after elution of the solvent that cannot be assigned to the expected regioisomers is assigned to impurities. The stated mole fractions of regioisomers do not consider the impurities, i.e. *x*_{ortho} + *x*_{meta} + *x*_{para} =

Table 1

– Specification of the self-made regioisomers of BT.

Substance	CAS number	Chemical structure	<i>M</i> /(g·mol ^{−1})	Share of <i>cis</i> isomer <i>x</i> _{cis} ^a	Purity ^b
H0-o-BT	713-36-0		182.26	–	0.980
H0-m-BT	620-47-3		182.26	–	0.989
H0-p-BT	620-83-7		182.26	–	0.979
H12-o-BT	<i>cis</i> : 54,824-04-3		194.36	0.3621	0.985
	<i>trans</i> : 54,823-94-8				
H12-m-BT	<i>cis</i> : 54,823-96-0		194.36	0.7404	0.985
	<i>trans</i> : 54,823-95-9				
H12-p-BT	<i>cis</i> : 54,823-97-1		194.36	0.3752	0.979
	<i>trans</i> : 54,823-98-2				

^a Mole fractions of the *cis* stereoisomers in H12-BT regioisomers determined by GC-FID analysis considering only the peaks of the two stereoisomers.

^b Purity determined by GC-FID analysis considering the peak areas of the corresponding regioisomers compared to all peaks after solvent elution obtained in the chromatogram.

1. Slight deviations between the fractions of ortho-, meta-, and para-isomers in H0-BT and H12-BT originate most probably from the use of a different sample batch of H0-BT for the catalytic hydrogenation compared to the one used for the investigation of thermophysical properties of the dehydrogenated mixture.

Before further use of the samples for investigations or for the preparation of mixtures, they were filtered using a polytetrafluoroethylene filter with a pore size of 0.2 μm to remove particle-like impurities and degassed under vacuum at *p* < 10 Pa and *T* ≈ 323 K. For sample storage and during most experiments, argon (Ar) purchased from Air Liquide S. A. with a mole fraction purity *y* of 0.99999 was used for creating an inert gas atmosphere. H₂ purchased from Linde plc of purity *y* = 0.999999 was employed for the investigation of its mixtures with H12-o-BT.

Using the pure regioisomers, further mixtures were created to systematically investigate the influence of mixture composition on the thermophysical properties of interest. The mixed samples are listed in Table 2 together with information on their regioisomeric composition in terms of *x* excluding impurities. The purities of the samples have only been considered after mixing for the calculation of the exact compositions stated here and, thus, the stated values may slightly deviate from the targeted ones. For the calculation of the composition as well as the amount of impurities in the mixtures based on the weighed masses of their components, the specified purities of the latter in terms of GC area

Table 2

– Specification of the investigated mixtures of different regioisomers.

Mixture name	H0-BT			H12-BT			Calculated/measured impurities $w_{\text{impurities}}$
	x_{ortho}^a	x_{meta}^a	x_{para}^a	$x_{\text{ortho}}^a (x_{\text{cis}})^b$	$x_{\text{meta}}^a (x_{\text{cis}})^b$	$x_{\text{para}}^a (x_{\text{cis}})^b$	
H0-o/p-25	0.250	–	0.750	–	–	–	0.021 ^c
H0-o/p-50	0.495	–	0.505	–	–	–	0.021 ^c
H0-o/p-75	0.750	–	0.250	–	–	–	0.020 ^c
H0-BT	0.4676	0.0539	0.4785	–	–	–	0.007 ^d
H0-BT _{mix}	0.468	0.054	0.478	–	–	–	0.020 ^c
H0-BT _{equi}	0.333	0.333	0.334	–	–	–	0.017 ^c
H12-o/p-50	–	–	–	0.494	–	0.506	0.018 ^c
H12-BT	–	–	–	0.4585 (0.4976)	0.0628 (0.7453)	0.4787 (0.3393)	0.009 ^d
H12-BT _{mix}	–	–	–	0.468	0.054	0.478	0.018 ^c
H12-BT _{equi}	–	–	–	0.333	0.334	0.333	0.017 ^c
o-BT-25	0.749	–	–	0.251	–	–	0.019 ^c
o-BT-50	0.499	–	–	0.501	–	–	0.017 ^c
o-BT-75	0.249	–	–	0.751	–	–	0.016 ^c

^a Mole fractions of regioisomers in the prepared mixtures calculated based on masses of mixture components using M of the pure samples neglecting impurities. Regioisomer mole fractions of H0-BT and H12-BT were directly measured by GC-FID excluding impurities.

^b Measured by GC-FID.

^c Calculated from the purities of the used samples of pure regioisomers considering their masses in the mixture.

^d Impurities measured by GC-FID in terms of peak area fractions.

fractions are assumed to be identical to mass fractions w . The calculated amount of impurities for the prepared mixtures is consequently given as $w_{\text{impurities}}$. The mixtures were prepared using a balance with a digit precision of 0.1 mg and an estimated total uncertainty of 1 mg. For readability purposes, the sample names of the mixtures prepared from the pure regioisomers are abbreviated. H0 and H12 indicate dehydrogenated and fully hydrogenated mixtures. The binary mixtures of ortho- and para-regioisomers are indicated with o/p followed by a number specifying the rounded mole fraction of the ortho-component in the mixture in percent. The shares of ortho- and para-isomers in the mixtures H0-o/p-50 and H12-o/p-50 have been adjusted to match those of H0-BT and H12-BT excluding the meta-isomer. H0-BT_{mix} and H12-BT_{mix} refer to ternary mixtures made from the regioisomers with compositions corresponding to those of H0-BT and H12-BT, while H0-BT_{equi} and H12-BT_{equi} represent ternary mixtures with equimolar shares of the regioisomers. For the binary mixtures of H0-o-BT and H12-o-BT, the number following “o-BT” specifies the rounded DoH in percent, which corresponds to the mole fraction of H12-o-BT.

2.2. Vibrating-tube densimetry (VTD) – liquid density

Liquid densities ρ_L at $p \approx 0.1$ MPa were measured by instruments from Anton Paar based on the vibrating-tube method. With the model DMA 5000 M, measurements with expanded (coverage factor $k = 2$) uncertainties of $U_r(\rho_L) = 0.02\%$ and $U(T) = 0.01$ K were performed from $T = (283.15 \text{ to } 363.15)$ K. The model DMA 4200 M was used for a broader T range with $U(T) = 0.03$ K, where measurements from $T = (298.15 \text{ to } 423.15)$ K and at $T = (448.15 \text{ and } 473.15)$ K are associated with uncertainties ($k = 2$) of $U_r(\rho_L) = (0.1 \text{ and } 0.2)\%$, respectively. While the general procedure of using the DMA 5000 M is the same as reported in Ref. [39], corresponding details including the calibration procedure for the DMA 4200 M are given in Ref. [35]. For measurements at the same T with both instruments, the results from the DMA 5000 M were always clearly within the uncertainty of those from the DMA 4200 M.

2.3. Pendant-drop (PD) method – surface or interfacial tension

The surface tension σ of the BT-based systems was studied under an Ar-rich atmosphere close to $p = 0.1$ MPa by the pendant-drop (PD) method. Here, the pure dehydrogenated and fully hydrogenated regioisomers, H0-BT, H12-BT, and the mixtures of H0-o-BT and H12-o-BT were studied between $T \approx (303 \text{ and } 523)$ K. All other systems were investigated from $T = (303 \text{ to } 423)$ K. Furthermore, the interfacial

tension σ of H12-o-BT under the influence of a H_2 atmosphere was examined between $T = (323 \text{ and } 423)$ K and at p up to 6 MPa. The latter study was carried out using the setup configuration detailed in Ref. [33], whereas for the investigation with an Ar atmosphere, the simplified configuration for measurements close to ambient p was employed [38, 39]. In the following, only the main information of the PD experiments is summarized. Further experimental details are given in section S3 of the Supporting Information.

At each investigated state point, at least 5 droplets were hung on the capillary tip with a typical equilibration time of about 10 min per droplet before taking the pictures to be analyzed. For the investigations with H_2 , σ of the first droplet was evaluated in time intervals of 5 min to check if the droplet was equilibrated. At $T > 423$ K, occasional shrinkage of the drop in the presence of an Ar atmosphere was compensated for by slight replenishing of liquid sample. For each droplet, 5 pictures were recorded in time steps of 10 s which were evaluated by applying axisymmetric drop-shape analysis [40–42] according to the procedure detailed in Ref. [39]. In short, theoretical drop shapes obtained by solving the Young-Laplace (YL) equation [43] were adjusted to match the detected droplet contour. The diameter of the capillary needed for the conversion from the pixel to the metric domain was calibrated prior to the experiments by means of a reference sphere. Details on the determination of the density difference between the liquid (ρ_L) and the gas (ρ_G) phase required for the solution of the YL equation are given in section S4 of the Supporting information.

The maximum relative deviation of σ obtained from the individual pictures from the corresponding average value at a specific state point was always less than the associated relative expanded uncertainty $U_r(\sigma) = 2\%$ up to 473 K and $U_r(\sigma) = 3\%$ at $T = 523$ K. On average, the T stability for all state points investigated under an Ar atmosphere was ± 4.0 mK, where the stability was always better than ± 8.5 mK at T up to 423 K and ± 14 mK above. Exceptions are given for o-BT-25 and o-BT-75 at $T = 523$ K, where the stabilities were better than $\pm(21 \text{ and } 24)$ mK. For the investigations with pressurized H_2 , the T stability was on average ± 6.3 mK and always better than $\pm(10 \text{ and } 12)$ mK for T up to 423 K and above. The p stability was always better than ± 20 kPa, with the exception of measurements at $T = 523$ K and $p = 3$ MPa, where the stability was better than ± 30 kPa.

2.4. Capillary viscometry (CV) – viscosity

CV measurements were performed with all samples listed in Table 1 and Table 2 to determine the liquid kinematic viscosity ν_L at T between (303 and 473) K and $p \approx 0.1$ MPa employing two setups. For the T range

between (303 and 353) K, measurements with an Ubbelohde capillary type 0a in a water bath were conducted at ambient atmosphere, while for $T = (353–473)$ K, measurements with an Ubbelohde capillary type 0c immersed in an oil bath were performed in the presence of an Ar atmosphere inside the capillary. The experimental setups and the calibration of the capillaries are described in detail in Refs. [44,45]. At a given T , five flow time measurements with a maximum relative deviation of 0.1% from their average were recorded. η_L values were calculated under consideration of the Hagenbach correction and using ρ_L data as described in section S4 of the Supporting Information. The results obtained at the same state point were ultimately averaged. For samples studied in both setups, the measurements at $T = 353$ K agreed mostly within 0.4% and always within 0.6%, where the unweighted average of the results is reported. The uncertainties ($k = 2$) of the calibrated Pt-100 resistance probes are $U(T) = 40$ mK for the setup used up to $T = 353$ K and $U(T) = 20$ mK for the setup used up to $T = 473$ K. The recorded T stability was better than $\pm(20$ and $40)$ mK up to (353 and 473) K during the measurements. Together with measured T variations along the capillary of less than ± 30 mK at $T = 473$ K, the overall uncertainty ($k = 2$) in the reported T is estimated to be $U(T) = 50$ mK up to $T = 353$ K and linearly increases to $U(T) = 80$ mK at $T = 473$ K. The procedure for estimating the uncertainty in η_L is described in detail in Ref. [45] and yields expanded ($k = 2$) relative uncertainties $U_r(\eta_L)$ between 0.7% at $T = 303$ K and 2.6% at $T = 473$ K.

Repetition measurements performed for the regioisomers as well as for H0-BT and H12-BT at lower T after the maximum T in the respective setups indicate thermal stability up to $T = 423$ K for all samples as well as up to $T = 473$ K for all H12-BT regioisomers and H0-m-BT. This can be deduced from the agreement of the results of the repetition and initial measurements considering the expanded uncertainties. For H0-o-BT, H0-p-BT, H0-BT, and H12-BT, however, the positive relative deviations of the repetition results from the previous measurements of (1.3, 1.8, 1.6, and 0.76)% after $T = 473$ K may indicate a limited thermal stability of these samples beyond 423 K, which might be related to the influence of small traces of air. Consequently, the measurement results for these samples at $T > 423$ K should be handled with care.

2.5. Surface light scattering (SLS) – surface or interfacial tension and viscosity

SLS was applied for the simultaneous determination of σ and η_L of the H0- and H12-BT regioisomers as well as of the mixture samples H0-BT, H12-BT, H0-BT_{mix}, H12-BT_{mix}, and H12-o/p-50 at T between in total (303 and 573) K at $p \approx 0.1$ MPa. Additionally, the influence of pressurized H_2 on σ and η_L was studied exemplarily for H12-o-BT at $T = (323, 423, \text{ and } 523)$ K and p up to 6 MPa. Relevant details on the theoretical principles [46,47] of this technique as well as its application for thermophysical property research [48,49] available in the given literature will be briefly summarized in the following.

By SLS, the dynamics of surface fluctuations at the phase boundary between two fluid phases at macroscopic thermodynamic equilibrium is analyzed by means of photon correlation spectroscopy. Here, the intensity of the light scattered by the phase boundary and modulated by the surface fluctuations, also known as capillary waves, with a defined modulus of the wave vector q is recorded as a function of time. This allows to calculate time-dependent intensity correlation functions (CFs) which reflect the temporal behavior of the studied surface fluctuations. For all studied samples, T , and q , the scattered light was detected in a heterodyne scheme in transmission direction perpendicular to the fluid interface. All recorded CFs revealed an oscillatory behavior associated with propagating waves. By representing the experimental CFs with the theoretical description of the dynamics of surface fluctuations without any viscoelastic behavior in the form of a damped oscillation [47], their characteristic dynamic parameters decay time τ_C or damping $\Gamma = 1/\tau_C$ and frequency ω_q are obtained. For reduced capillary numbers $Y < 20$, an additional contribution in the signal originating from the rotational

flow in the bulk of the fluid [46,47,50] is considered according to the procedure described in Ref. [51]. σ and η_L are determined by numerically solving the dispersion equation $D(\eta_L, \eta_G, \rho_L, \rho_G, \sigma, \Gamma, \omega_q, q)$ for capillary waves between a liquid (index L) and a gas (index G) phase without the presence of viscoelastic effects [46–48]. Information on ρ_L , ρ_G , and η_G required as input are given in section S4 in the Supporting Information.

The experimental setup used to perform SLS measurements in this study is the same as that described in Ref. [34]. Relevant information about the experimental procedure and the measurement conditions can be found in section S3 of the Supporting Information. The reported values for σ and η_L represent the unweighted averages of the results obtained from the six individual measurements at different q . Corresponding uncertainties have been evaluated according to the error propagation scheme described in Ref. [52] based on the reproducibility of the individual measurements and the uncertainties of the input parameters.

For experiments with pressurized H_2 , p was stepwise adjusted at a given T between (0.1, 3.0, and 6.0) MPa. Here, a p transducer with an expanded ($k = 2$) uncertainty $U(p) = 5$ kPa was employed to monitor p inside the sample cell. The p stability during experiments with H_2 was always better than $\pm(11$ and $22)$ kPa at $p = (3.0$ and $6.0)$ MPa. Based on the measured p , H_2 concentrations in the saturated liquid phase x_{H_2} are calculated using solubility data from Ref. [53] as detailed in section S4 of the Supporting Information.

2.6. Dynamic light scattering (DLS) from the bulk of the fluid – Thermal and Fick diffusivities

Details about the underlying theory of DLS applied to the bulk of fluids for the simultaneous determination of the thermal diffusivity a and the Fick diffusion coefficient D_{11} as well as its application in thermophysical property research given in the cited literature [54–56] will be summarized in the following, with focus on the essential aspects related to the present experiments. By DLS, the dynamics of statistical fluctuations in T and concentration in the bulk of a binary fluid mixture at macroscopic thermodynamic equilibrium is probed. The analysis of the scattered light intensity for a defined q gives information about the temporal behavior of these fluctuations, from which a and D_{11} can be obtained. The corresponding CFs recorded in a heterodyne detection scheme and analyzed via photon correlation spectroscopy could be described by the sum of two exponentially decaying modes related to hydrodynamic fluctuations. The obtained characteristic decay times or mean life times of the fluctuations in T and concentration, $\tau_{C,t}$ and $\tau_{C,c}$, are related to a and D_{11} according to

$$a = (\tau_{C,t} q^2)^{-1} \text{ and } D_{11} = (\tau_{C,c} q^2)^{-1}. \quad (1)$$

DLS measurements were performed in the bulk of the saturated liquid phase of H12-o-BT containing dissolved H_2 at $p = 6.0$ MPa and $T = (323, 423, \text{ and } 523)$ K after the SLS experiments at the corresponding state points. Further DLS experiments were carried out at $T = (373$ and $473)$ K and $p = 6.0$ MPa using the same experimental setup. Details on the experimental procedure and the measurement conditions are provided in section S3 of the Supporting Information. The values reported for a and D_{11} are the averages of the results obtained for the twelve individual CFs according to Eq. (1), which are weighted by their inverse relative statistical uncertainty being dominated by the fit uncertainty in the respective τ_C . For $T = (473$ and $523)$ K, a Lewis number $Le = a/D_{11}$ close to unity as well as a limited signal-to-noise ratio in the recorded CFs made it impossible to resolve both exponentially decaying modes individually. Here, the CFs can only be described by a single exponential decay resulting in a mixed diffusivity D_{mix} associated with both a and D_{11} . As related uncertainties can hardly be quantified, no corresponding values are specified.

3. Results and discussion

For readability purposes, the index L representing the liquid phase will be omitted in the following discussions on the liquid density and liquid viscosity.

3.1. Liquid density

The experimental results for the liquid density ρ of the studied samples measured at ambient atmosphere are given in Tables S3 and S4 in the Supporting Information. The experimental results for ρ of the H0- and H12-BT regioisomers, of H0-BT and H12-BT as well as of the binary mixtures of H0-o-BT and H12-o-BT are represented as a function of T in Fig. 1. Data for the further mixtures of H0- or H12-BT regioisomers are not included here to ensure legibility.

For ρ of the regioisomers, H0-BT and H12-BT, and the binary mixtures of H0-o-BT and H12-o-BT with varying DoH , T -dependent correlations have been obtained by unweighted fitting of the experimental data according to

$$\rho_{\text{calc}}(T) = \rho_0 + \rho_1 T + \rho_2 T^2, \quad (2)$$

where the experimental data could be described within their uncertainties. The fit parameters ρ_0 , ρ_1 , and ρ_2 in Eq. (2) are given together with the average absolute relative deviation (AARD) of the measured data from their fit in Table S5 in the Supporting Information.

3.1.1. Pure regioisomers

Fig. 1 shows that with increasing T , ρ of all samples decreases from $T = (283 \text{ to } 473) \text{ K}$ by (14–15)%, while ρ of the H12-BT regioisomers is by (12 and 13)% smaller than that of their dehydrogenated counterparts at $T = (283 \text{ and } 473) \text{ K}$. The behavior of ρ is very similar for the structurally related LOHC systems based on DPM [38] or DBT [32], where ρ of the hydrogenated species is by (12–13)% smaller than for their dehydrogenated counterparts at a given T . Also the relative decrease of ρ of the DPM- or DBT-based substances with increasing T corresponds to that of the BT-based regioisomers for comparable T ranges. For both the hydrogenated and the dehydrogenated case, the ρ values of the different regioisomers show small, yet measurable differences of up to about 1.5%. Hence, these relative differences are less pronounced than those of up to 2.2% found for the xylene regioisomers by Al-Kandary et al. [26].

To discuss the differences in ρ between the regioisomers in detail, the relative deviations of the experimental data from the fits of the

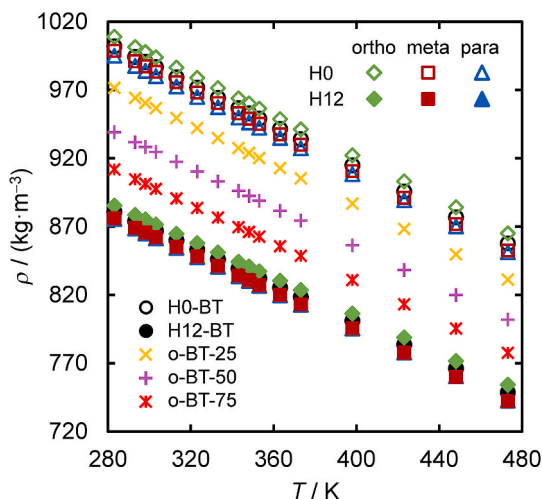


Fig. 1. Experimental liquid density data for the H0- and H12-BT regioisomers, H0-BT and H12-BT, and the binary mixtures of H0-o-BT and H12-o-BT as a function of T . (For interpretation of the references to color in this figure legend, the reader is referred to the Web version of this article.)

corresponding technical mixtures $\rho_{\text{calc,H0-BT}}$ and $\rho_{\text{calc,H12-BT}}$ according to Eq. (2) are represented in Fig. 2 for the dehydrogenated (left) and the fully hydrogenated (right) case as a function of T . Here, also the results for the binary and ternary mixtures prepared from the regioisomers to be discussed later on as well as experimental data from the accessible literature for H0-o-BT [27], H0-m-BT [27,28], and H0-p-BT [27,29–31] and for the *cis* and *trans* stereoisomers of H12-o-BT, H12-m-BT, and H12-p-BT [27] are included. In Fig. 2 and in all following figures of this work, error bars represent the experimental expanded ($k = 2$) uncertainties and are only included exemplarily for some data sets to ensure legibility.

Among the H0-BT regioisomers, H0-o-BT exhibits the largest ρ , while the values for the meta- and para-isomers are up to (1.4 and 1.6)% smaller. Here, the relatively small distance between the methyl and the methylene group in the case of the ortho-isomer seems to allow for a considerably closer packing of the molecules compared to the meta- and para-isomers. This picture is supported by the fact that the same order regarding ρ is reported for the three regioisomers of xylene [26]. The ρ values from Lamneck and Wise [27] for H0-o-BT, H0-m-BT, and H0-p-BT at $T = 293.15 \text{ K}$ only deviate by (+0.05, +0.03, and −0.02)%, respectively, from the present results, while the other literature sources report somewhat larger ρ data. For H0-m-BT, Senff [28] obtained a by 0.4% larger value. For H0-p-BT, the previously reported data are between (0.5 and 1.0)% larger than the present results [29–31].

Considering the right part of Fig. 2, the ρ data of the H12-BT regioisomers take the same order as in the dehydrogenated case. Similarly, ρ of H12-p-BT is by up to 1.6% smaller than that of H12-o-BT. Compared to the dehydrogenated isomers, ρ of H12-m-BT shows relatively small differences to H12-p-BT, which are less than 0.1%. The data reported by Lamneck and Wise [27] at $T = 293.15 \text{ K}$ relate to the isolated *cis* and *trans* stereoisomers of the three regioisomers, which have only been marked as high-boiling and low-boiling isomers in their work. In Fig. 2, their samples were assigned to *cis* and *trans* assuming that the order of boiling points specified by Lamneck and Wise [27] is in accordance with the elution order in the GC. While for the ortho- and para-regioisomers, the *cis* conformation exhibits a larger ρ than the corresponding *trans* counterpart, this behavior is inverted for the meta-regioisomer. For a more direct comparison, the mixing rule given in Eq. (3) was applied to the data from Lamneck and Wise [27] using the stereoisomeric compositions for the present samples of H12-o-BT, H12-m-BT, and H12-p-BT reported in Table 1. The calculated values show relative deviations of (−0.03, +0.02, and −0.01)%, respectively, from the present results measured for the stereoisomeric mixtures, which is clearly within combined uncertainties. Although this might indicate that the employed mixing rule can be applied to predict ρ of arbitrary stereoisomeric mixtures of H12-BT regioisomers, more data for ρ of the pure stereoisomers and their mixtures would be required to support this assumption.

3.1.2. Mixtures of H0-BT or H12-BT regioisomers

The agreement within single experimental uncertainties between the ρ data for the regioisomer mixtures H0-BT and H0-BT_{mix} shown on the left side of Fig. 2 indicates a negligible influence of the different quantities and types of impurities contained in H0-BT_{mix} prepared from the synthesized regioisomers compared to the commercial mixture H0-BT. ρ of H0-o/p-50 also shows negligible deviations from ρ of H0-BT and H0-BT_{mix}, which highlights an insignificant influence of the meta-isomer in the ternary mixtures at the given concentration of $x_{\text{H0-m-BT}} = 0.054$. The equimolar mixture of the three regioisomers, H0-BT_{equi}, exhibits by about 0.1% smaller values for ρ than H0-BT and H0-BT_{mix}. This behavior is related to a decrease in $x_{\text{H0-o-BT}}$ having the highest ρ and an increase in the sum of $x_{\text{H0-m-BT}}$ and $x_{\text{H0-p-BT}}$ exhibiting smaller ρ than the aforementioned ternary mixtures.

On the right side of Fig. 2, the mixture H12-BT_{mix} shows relative deviations in ρ from the fit for H12-BT of up to −0.07%, which is outside combined measurement uncertainties ($k = 2$) of the used DMA 5000 M

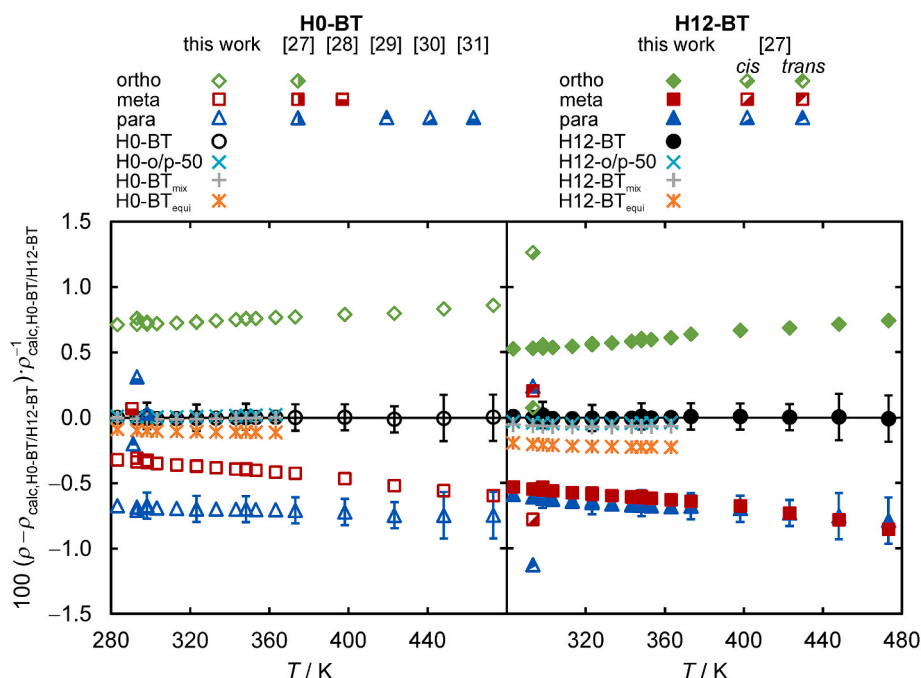


Fig. 2. Relative deviations of experimental ρ values for the pure BT regioisomers and their binary and ternary mixtures as well as H0-BT and H12-BT from the T -dependent correlation of the technical mixtures as a function of T in the dehydrogenated (left) and fully hydrogenated (right) case. In addition, experimental data for the pure regio- or stereoisomers available in the literature [27–31] are included. (For interpretation of the references to color in this figure legend, the reader is referred to the Web version of this article.)

densimeter. This significant deviation despite corresponding regioisomeric composition may be explained by the differences in the stereoisomeric composition of the synthesized regioisomers used for mixing H12-BT_{mix} compared to H12-BT, which is related to slightly different reaction conditions during hydrogenation. Consequently, a direct comparison of the further studied mixtures obtained from the synthesized regioisomers with H12-BT is not possible. In comparison to the self-mixed H12-BT_{mix}, H12-o/p-50 shows by 0.03% larger values, which is within combined experimental uncertainties and reflects a relatively weak influence of the meta-isomer at the given concentration in H12-BT_{mix}. For the equimolar mixture H12-BT_{equi}, however, relative deviations of the ρ data from those of H12-BT_{mix} of up to -0.16% are observed. Overall, the relative trends in ρ of the fully hydrogenated regioisomers and their mixtures are similar to those for the dehydrogenated cases. The data from Müller et al. [32] for isomeric mixtures of H0-BT and H12-BT were excluded from the comparison in the left and right side of Fig. 2 due to the missing specification of the isomeric composition.

For all dehydrogenated and fully hydrogenated mixtures prepared from the regioisomer samples, the experimental ρ data can be represented well by a simple mixing rule using the definition of the excess molar volume V_m^E according to

$$\rho_{\text{mix}} = \frac{\sum_i x_i M_i}{V_m^E + \sum_i \frac{x_i M_i}{\rho_i}} \quad (3)$$

For $V_m^E = 0$, Eq. (3) can estimate ρ_{mix} of the dehydrogenated or fully hydrogenated mixtures consisting of the synthesized H0- or H12-BT regioisomers using ρ_i for the pure regioisomers calculated according to Eq. (2) as well as their mole fractions x_i and molar masses M_i . Treating the H12-BT regioisomer samples as pure mixture components despite the stereoisomerism, an AARD of 0.022% of the molar volume-based estimation from the experimental values considering all T are found. When the mixture H12-BT_{mix} is excluded, the AARD reduces to 0.0049%.

3.1.3. Mixtures of H0- and H12-ortho-BT with varying DoH

To study the mixture behavior of ρ for the BT-based system as a function of the DoH, three quasi-binary mixtures of H0-o-BT and H12-o-BT have been investigated exemplarily. Applying the mixing rule of Eq. (3) with $V_m^E = 0$ and using ρ_{calc} obtained from Eq. (2) for pure H0-o-BT and H12-o-BT results in AARDs of (0.20, 0.24, and 0.03)% from the corresponding experimental values for o-BT-25, o-BT-50, and o-BT-75, respectively, considering the full T range. This finding indicates a slightly non-ideal mixing behavior of the dehydrogenated and fully hydrogenated species with $V_m^E \neq 0$, which is, however, of rather insignificant importance for technical applications. In Fig. 3, the calculated V_m^E data of the mixtures are represented as a function of the DoH for $T =$

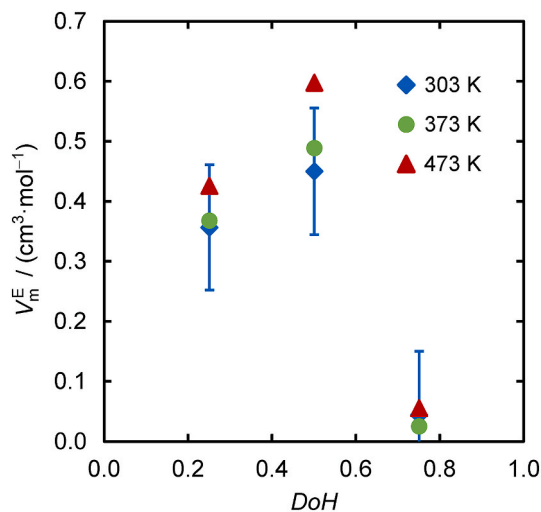


Fig. 3. Excess molar volume of quasi-binary mixtures of H0-o-BT and H12-o-BT as a function of the DoH at selected T . (For interpretation of the references to color in this figure legend, the reader is referred to the Web version of this article.)

(303, 373, and 473) K. Error bars are not included for $T = (373 \text{ and } 473)$ K because here, the relative uncertainties obtained by error propagation are always larger than (80 and 155)%. A maximum V_m^E of about $+0.6 \text{ cm}^3 \text{ mol}^{-1}$ can be observed for $DoH = 0.50$. This positive value indicates that for the present mixtures, the intermolecular interactions between unlike species seem to be weaker than those between the two mixture components in their pure forms. This apparently reduces the packing density of the molecules in the mixtures compared to an ideal mixing behavior. Similar results regarding the magnitude and the DoH -dependent trend of the V_m^E have already been reported for other binary or quasi-binary mixtures of aromatic compounds and their hydrogenated derivatives such as H0-DPM and dicyclohexylmethane (H12-DPM) [38], H0-DBT and perhydrodibenzyltoluene (H18-DBT) [57], benzene and cyclohexane [58,59], or toluene and methylcyclohexane [60].

3.2. Surface or interfacial tension

The experimental results for the surface tension σ of the H0- and H12-BT regioisomers as well as the studied mixtures in the presence of an Ar atmosphere at $p \approx 0.1 \text{ MPa}$ obtained by the PD method up to $T = 523 \text{ K}$ and by SLS up to $T = 573 \text{ K}$ are summarized in Tables S6 and S7 in the Supporting Information. The results for the interfacial tension σ of H12-o-BT in the presence of pressurized H_2 at varying T and p obtained from the PD method and SLS are given in Tables S8 and S9, together with the related data for x_{H_2} . The individual SLS data for σ and the dynamic viscosity η , which are presumably influenced by viscoelastic effects at the vapor-liquid interface, as will be discussed in the following, are only apparent results and are marked in Tables S7 and S9.

The data for σ of the pure regioisomers, H0-BT and H12-BT, and binary mixtures of H0-o-BT and H12-o-BT measured in Ar atmosphere by the PD method were correlated by a T -dependent fit according to

$$\sigma_{\text{calc}}(T) = \sigma_0 + \sigma_1 T + \sigma_2 T^2 \quad (4)$$

using the same statistical weight for all data points in a least-squares minimization algorithm. The values for the fit coefficients σ_0 , σ_1 , and σ_2 describing the data within their experimental uncertainties as well as the AARDs of the experimental data from their fit are given in Table S10 in the Supporting Information.

Considering the challenges in using SLS for bicyclic hydrocarbons, which have partially been observed in recent investigations for the LOHC system based on DPM [38] or its mixtures with fluorene [45], it is necessary to compare the σ results obtained by SLS and the PD method before a comprehensive discussion of the data for the BT-based LOHC

system is performed. For this purpose, Fig. 4 shows the relative deviations of the results for σ determined via SLS from σ_{calc} of the corresponding samples according to Eq. (4) based on the results from the PD method as a function of T . Here, the results for the dehydrogenated regioisomers and H0-BT as well as for the fully hydrogenated regioisomers and H12-BT are given separately. While to the best of the authors' knowledge, no σ data for the pure regioisomers have been published in the literature that could be used for comparison purposes, Müller et al. [32] studied a commercially available mixture in the dehydrogenated and fully hydrogenated state. This study is, however, not useful for the present data comparison due to the missing information on the isomeric composition of the samples. The relative deviations between the SLS and PD data are mostly within 5% and often within combined uncertainties considering the experimental uncertainties of the PD data of 2% up to $T = 473 \text{ K}$ and 3% above, indicated by the dashed lines in Fig. 4. Clearly larger deviations are observed especially at low T for H0-o-BT and H12-o-BT, where the SLS results are up to 13% lower than the data obtained from the PD method. Yet, these relative deviations decrease steadily with increasing T to less than (2–3)% at $T \geq 423 \text{ K}$. For all samples and T , the SLS results for σ are lower than the data from the PD method. The significant differences especially for H0-o-BT and H12-o-BT are accompanied by an unusual T -dependent behavior of σ obtained by SLS and can be explained by the relatively high sensitivity of this technique to surface-active impurities.

It has already been shown in the literature that for fluids containing highly asymmetric surfactant molecules, the apparent values for σ obtained by SLS from the evaluation of the dispersion relation of surface fluctuations neglecting any viscoelastic behavior are typically lower than those measured by conventional techniques [61–63]. Recently, it could be demonstrated for the DPM-based LOHC system that the partially hydrogenated reaction intermediate cyclohexylphenylmethane (H6-DPM) acts as a weakly asymmetric surfactant and induces a viscoelastic behavior in its mixtures with H0-DPM [64]. In this case, where H6-DPM shows only a slightly lower surface tension than H0-DPM, the apparent results for the mixture obtained by SLS are significantly influenced already at a small H6-DPM mole fraction of $x_{H6-DPM} = 0.001$. In contrast, the results from conventional techniques like the PD method remained almost unaffected. Also there, the observed influence on σ was most pronounced at low T and decreased with increasing T , which can be associated with increasing molecular dynamics in the fluid and weakened accumulation of the impurities at the vapor-liquid interface. For the present sample of H0-o-BT, the GC analysis revealed that isomers of methylcyclohexyl-methylbenzene (H6-BT) constitute the major

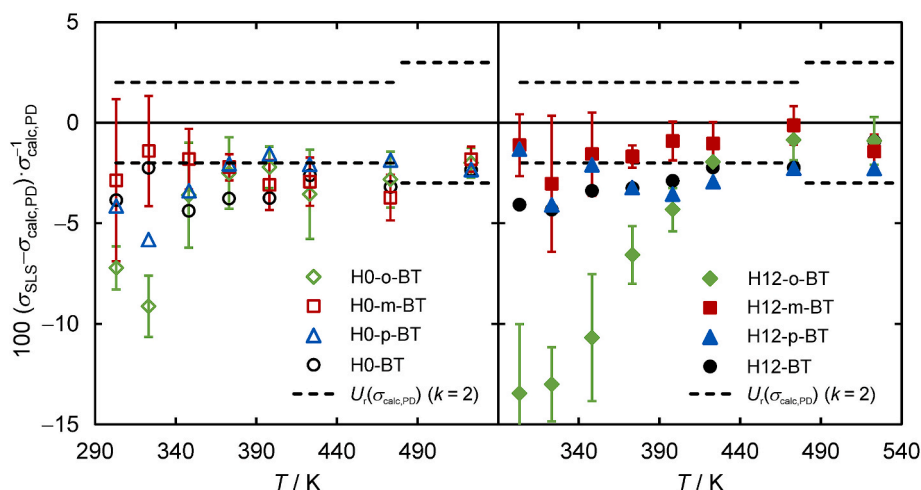


Fig. 4. Relative deviation of σ values obtained by SLS for regioisomers and the technical mixture of BT in dehydrogenated (left) and fully hydrogenated (right) form from corresponding values measured by the PD method. The dashed lines represent the experimental uncertainty ($k = 2$) of the PD data. (For interpretation of the references to color in this figure legend, the reader is referred to the Web version of this article.)

impurity with $x_{\text{H6-BT}} = 0.013$, from which a similar influence as for the DPM-based system can be anticipated. Compared to that, the considerably smaller mole fractions of H6-BT in H0-m-BT, H0-p-BT, and H0-BT of $x_{\text{H6-BT}} = (0.003, 0.003, \text{ and } 0.001)$ are consistent with the smaller negative deviations of the corresponding apparent SLS data from the PD results. In the H12-o-BT sample, no H6-BT was found, but unidentified high-boilers observed by GC might act as surface-active impurities. Due to the observed discrepancies and the identified influence of traces of impurities in SLS experiments, impeding also the interpretation of the mixture behavior of different BT isomers, the following discussion is mainly based on the results from the PD method. Nevertheless, it should be emphasized that the present SLS results provide reliable data for σ of the hydrogenated systems except for H12-o-BT and, for all investigated samples, especially at elevated T where they extend the data range up to 573 K.

3.2.1. Pure regioisomers and mixtures of H0-BT or H12-BT regioisomers

In Fig. 5, the PD results for σ of the H0- and H12-BT regioisomers are presented together with those for H0-BT and H12-BT as well as for mixtures of H0-o-BT and H12-o-BT as a function of T . The dehydrogenated H0-BT regioisomers show by about (20 and 30)% larger σ values than the fully hydrogenated ones at $T = (303 \text{ and } 523) \text{ K}$. This is in accordance with the behavior for pairs of bicyclic or tricyclic aromatic compounds and their hydrogenated counterparts, such as H0-DPM and H12-DPM [33] or H0-DBT and H18-DBT [32]. In a similar way as for the behavior regarding ρ , it can be explained by stronger dispersive intermolecular interactions related to the aromatic rings including π - π stacking interactions. At a given DoH , the relative differences between σ of the regioisomers are within 4%.

A more detailed resolution of the regioisomer-dependent behavior of σ can be seen in Fig. 6, where the relative deviations of σ of the pure regioisomers as well as their mixtures from the T -dependent correlation for H0-BT or H12-BT according to Eq. (4) are shown for the dehydrogenated (left) or the fully hydrogenated case (right). In both diagrams, nearly all data points of the individual samples agree within combined uncertainties. Analogously to the findings for ρ , the ortho-isomers tend to exhibit the largest σ values among the regioisomers of a given DoH , while those of the meta- and para-isomers are relatively similar. The same order with respect to σ as observed for the dehydrogenated isomers has also been reported for the regioisomers of xylene [65]. Nevertheless, deducing any relations between the σ results and the molecular structure

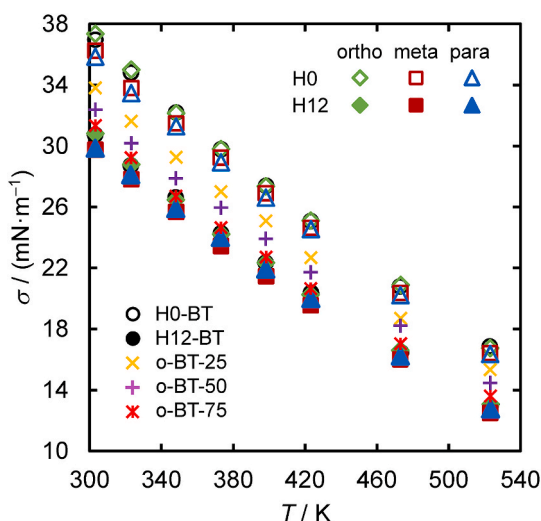


Fig. 5. Surface tension σ of the dehydrogenated and hydrogenated BT regioisomers, H0-BT and H12-BT as well as mixtures of H0-o-BT and H12-o-BT from the PD method as a function of T . (For interpretation of the references to color in this figure legend, the reader is referred to the Web version of this article.)

would be rather speculative considering the small differences and the measurement uncertainties. This also holds for the results for the dehydrogenated and fully hydrogenated mixtures prepared from the pure regioisomers, where the corresponding measured σ values are within the small range covered by the mixture components. Therefore, establishing specific mixing rules for σ is not reasonable. As H0-BT_{mix} and H12-BT_{mix} exhibit very similar σ values as H0-BT and H12-BT, a negligible influence of different amounts and types of impurities in the self-made and commercial mixtures can be concluded.

3.2.2. Mixtures of H0- and H12-ortho-BT with varying DoH

To investigate the DoH -dependent behavior of σ in the BT-based LOHC system, three quasi-binary mixtures of H0-o-BT and H12-o-BT were studied by the PD method. The results for the two regioisomers and their mixtures at $T = (303, 373, \text{ and } 473) \text{ K}$ are shown in Fig. 7 as a function of the DoH which is identical with $x_{\text{H12-o-BT}}$. For all T , a nonlinear decrease with increasing DoH is evident, where a steeper trend is visible at low DoH . This rather typical composition-dependent behavior for binary mixtures of components with different σ has also been reported for the structurally similar pair of H0-DPM and H12-DPM, where complementary molecular dynamics simulations have indicated an enrichment of the fully hydrogenated species with lower σ at the interface [38]. The surface enrichment becomes weaker with increasing T due to the intensified molecular motion, which is also reflected in the present results. For describing the DoH -dependent behavior of σ for the given mixtures of H0-o-BT and H12-o-BT, several approaches have been tested, where the stereoisomeric mixture H12-o-BT is regarded as a pure mixture component. Like for the mixtures of H0-DPM and H12-DPM [38], the empirical model of Vakili-Nezhaad et al. [66,67] calculating σ_{mix} of the mixtures according to

$$\sigma_{\text{mix}} = \frac{25RT}{3A} \left\{ 1 - \left[\sum_{i=1}^N x_i \left(1 - \frac{3\sigma_i A}{25RT} \right)^{25/3} \right]^{3/25} \right\} \quad (5)$$

showed the best representation of the DoH -dependent behavior. Here, R denotes the universal gas constant and x_i and σ_i are the mole fraction and surface tension of the pure components i . A is obtained by

$$A = 1.02 \times 10^8 \sum_{i=1}^N x_i V_i^{2/3} \quad (6)$$

with the molar volumes V_i of the mixture components calculated with the help of the correlations ρ_{calc} according to Eq. (2). For the three binary mixtures considering all studied T , the AARD of the predicted values σ_{mix} from the experimental PD results is 2.5%. For comparison, the model proposed by Goldsack and Sarvas [68], based on which the model suggested by Vakili-Nezhaad et al. [66,67] was developed, yields an AARD of 3.0%. Both models show a better performance than simple linear and logarithmic mixing rules based on mole fraction or mass fraction with AARDs $\geq 3.6\%$.

3.2.3. H12-o-BT in the presence of pressurized H₂

Fig. 8 shows the relative deviations of the PD and SLS results obtained for σ of H12-o-BT with dissolved H₂ at a given T and varying p from corresponding reference values measured with the same method under an H₂ atmosphere at $p \approx 0.1 \text{ MPa}$, $\sigma_{0.1 \text{ MPa}}$, for $T = (323, 423, \text{ and } 523) \text{ K}$. In the left and right part of Fig. 8, the deviations are represented as a function of the total pressure p and of x_{H2} calculated using solubility data from the isochoric-saturation method [53]. For the corresponding discussion, note that x_{H2} tends to increase linearly with increasing p at a given T as given in Tables S8 and S9. Furthermore, x_{H2} increases with increasing T at a defined p and is by a factor of about two larger at 523 K than at 323 K.

Both representations in Fig. 8 indicate agreeing tendencies of the PD and SLS data despite the previously discussed discrepancies between absolute σ values for H12-o-BT in Ar atmosphere. Here, the discussed

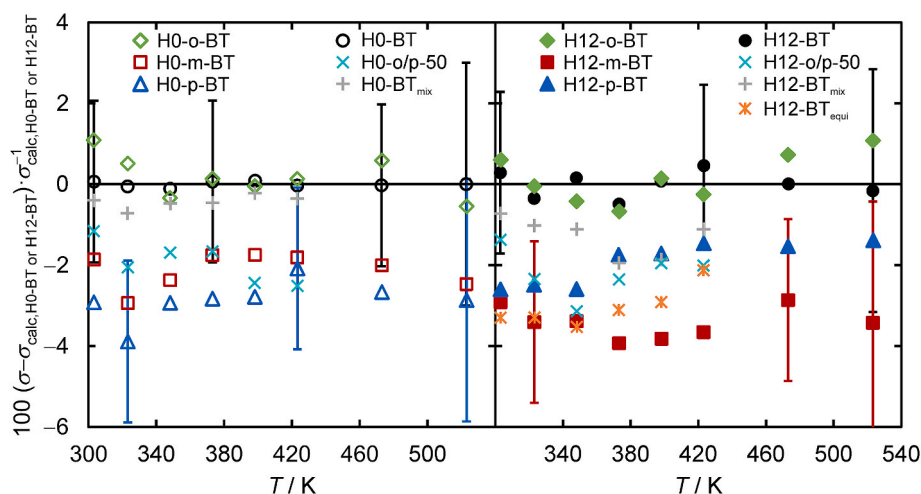


Fig. 6. Relative deviations of σ values of the dehydrogenated (left) and fully hydrogenated (right) regioisomers and corresponding mixtures thereof measured by the PD method from σ_{calc} of H0-BT and H12-BT calculated according to Eq. (4) as a function of T . (For interpretation of the references to color in this figure legend, the reader is referred to the Web version of this article.)

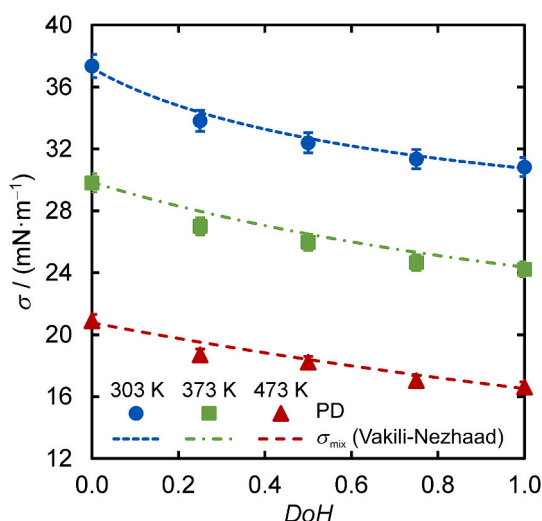


Fig. 7. Surface tension σ of H0-o-BT and H12-o-BT and their binary mixtures measured by the PD method as well as σ_{mix} calculated with the model of Vakili-Nezhaad et al. [66,67] according to Eq. (5) as a function of the DoH for selected T . (For interpretation of the references to color in this figure legend, the reader is referred to the Web version of this article.)

influence of impurities in the H12-o-BT sample on the SLS results mainly due to viscoelastic surface effects seems to be independent of p and x_{H_2} and consequently cancel out in the relative representation of σ as a function of p or x_{H_2} in Fig. 8. Thus, the relative change of σ compared to the reference value at $p \approx 0.1$ MPa according to the SLS data is equivalent to that found from the PD method. According to the left side of Fig. 8, σ decreases with increasing p by up to 5% at 6.0 MPa, where no clear difference between different T can be observed. On the right side of Fig. 8, the relative decrease in σ with increasing x_{H_2} up to about 0.09 seems to vary for the different T . While for the SLS data no clear T -dependent behavior is evident, the data obtained by the PD method indicate that the decrease in σ for a given x_{H_2} is most pronounced at the lowest T and becomes smaller with increasing T . Although it is within combined uncertainties of the σ data, this effect may be related to varying H_2 concentrations at the vapor-liquid interface with varying T despite a constant x_{H_2} in the bulk of the liquid. For DPM-based substances and mixtures with dissolved H_2 , it has been shown by molecular dynamics simulations that H_2 tends to enrich at the interface [34],

which can be assumed to apply for H_2 in combination with H12-o-BT as well. As this enrichment weakens with increasing T due to the intensified molecular motion [69], the resulting reduction of σ at a given x_{H_2} becomes less pronounced. Similar observations for the influence of H_2 on σ as a function of p have been reported for DPM-based solvents with a relative decrease of up to about 6% at 7 MPa [34]. Considering H_2 solubility data for the DPM-based solvents [33,53], a similar x_{H_2} -dependent behavior as shown here for H12-o-BT can be inferred for the DPM-based system. Beyond this LOHC system, the effect of pressurized H_2 on σ has only been studied for a few organic solvents so far. For methanol, a relative decrease by about 6% at $p = 8$ MPa compared to the reference values without the influence of H_2 was measured for T between (303 and 393) K [70]. Here, the x_{H_2} -dependent trends show the same T dependence as for H12-o-BT or the DPM-based systems. For ethanol and diethyl ether, a decrease by about (5 and 7)% at $p = 5$ MPa [71] has been observed without any specification on x_{H_2} . For n -hexane [72], n -hexadecane [69], n -octacosane [73], and 1-hexadecanol [73], a decrease in σ by up to about (10, 9, 5, and 4)% at 7 MPa compared to corresponding values at about 0.1 MPa have been reported. For the latter three systems studied at T between (298 and 573) K, a very weak x_{H_2} -dependent behavior as a function of T can be identified which, in accordance with the present findings based on the PD data, shows a decreasing influence of x_{H_2} with increasing T .

3.3. Dynamic viscosity

The experimental data for the liquid dynamic viscosity η of the pure regioisomers and isomeric mixtures obtained from SLS and CV at $p \approx 0.1$ MPa and T up to (573 and 473) K are given in Tables S7 and S11 in the Supporting Information. Therein, the SLS results for η of H12-o-BT in the presence of pressurized H_2 are summarized in Table S9 at varying T and p , corresponding to the specified x_{H_2} data. Based on the CV data for η of the regioisomers as well as of H0-BT and H12-BT, T -dependent correlations $\eta_{\text{calc}}(T)$ were calculated according to

$$\eta_{\text{calc}}(T) = \eta_0 \cdot \exp \left(\sum_{i=1}^3 \frac{\eta_i}{T^i} \right) \quad (7)$$

by a least-squares minimization algorithm. For fitting, the experimental results were represented by $\ln(\eta / \text{mPa}\cdot\text{s})$ versus (T^{-1} / K^{-1}) applying the same statistical weight for all data points. The fit parameters η_0 , η_1 , η_2 , and η_3 obtained from Eq. (7) for the individual samples are given in Table S12 of the Supporting Information and allow to represent all experimental data between $T = (303 \text{ and } 473) \text{ K}$ well within the

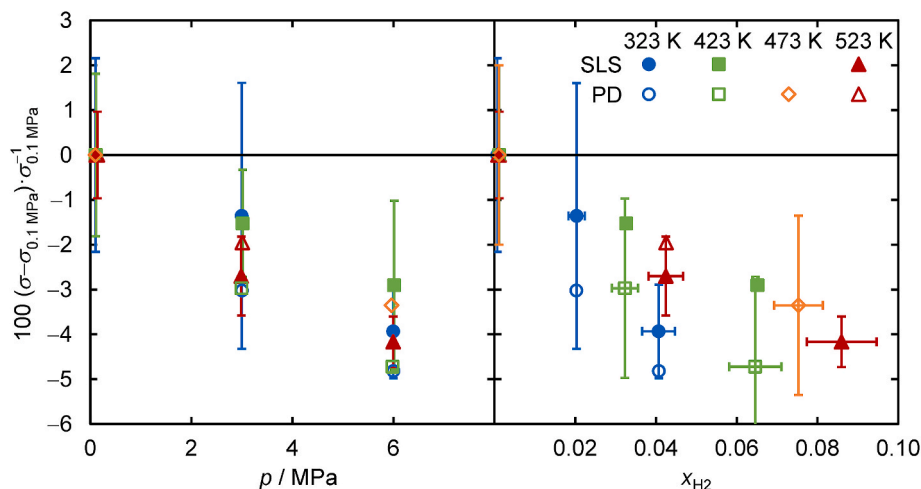


Fig. 8. Relative deviations of σ measured by the PD method and SLS for H12-o-BT in the presence of a H_2 atmosphere from corresponding values at $p \approx 0.1$ MPa for different T as a function of p (left) and as a function of x_{H_2} calculated using solubility data from Ref. [53] (right). (For interpretation of the references to color in this figure legend, the reader is referred to the Web version of this article.)

experimental ($k = 2$) uncertainties.

For the same purpose as in the section 3.2, Fig. 9 shows the relative deviations of η values obtained by SLS for the dehydrogenated regioisomers and H0-BT (left) as well as for the fully hydrogenated regioisomers and H12-BT (right) from the fit of the corresponding CV data according to Eq. (7) as a function of T . In the dehydrogenated case, the SLS results are generally larger than those from CV. While the results from both techniques at $T = 303$ K typically agree within combined uncertainties, the deviations mostly increase with increasing T and show a maximum at T between (348 and 398) K. Only for H0-BT, the relative deviations of the SLS values from η_{calc} based on CV data remain within 5% up to $T = 423$ K, whereas at $T = 473$ K, the SLS results are by 16% larger. The considerable deviations of the apparent viscosity data obtained by SLS from the CV results go along with pronounced systematics in the residuals between the recorded CFs and the theoretical fit model neglecting viscoelasticity at the interface. The latter phenomenon influences the temporal behavior of the studied surface waves and seems to be the reason for the observed systematics. As already discussed in connection with the results for σ , these viscoelastic effects are probably related to small amounts of H6-BT in the samples which acts here as surface-active impurity and may form a Gibbs monolayer at the surface

as found for H6-DPM in H0-DPM [64]. The monolayer induces an additional damping contribution to the dynamics of the surface waves. This leads to apparent η values determined by SLS which are significantly larger than the actual viscosity of the bulk liquid phase measured by conventional techniques such as CV. The magnitude of this viscoelastic effect strongly depends on the concentration of the surface-active species at the surface and appears to exhibit a maximum for system-specific, typically relatively small surface concentrations. Thus, the T -dependent maxima of the relative deviations of the SLS data from the CV results mostly observed here may be explained by the varying concentration of surface-active species in the surface region with varying T .

In the fully hydrogenated case given on the right side of Fig. 9, the SLS data mostly agree with the CV results within combined uncertainties and, with the exception of H12-o-BT, always within $\pm 6\%$. This relatively good agreement can mainly be associated with the absence of H6-BT, which is also not expected to accumulate at the surface of the fully hydrogenated samples exhibiting lower σ [64]. A matching of the SLS with the CV data could also be found for mixtures of H12-DPM with H6-DPM [64] or H0-DPM [38]. The considerably larger deviations of the SLS data for H12-o-BT at T between (348 and 423) K are probably

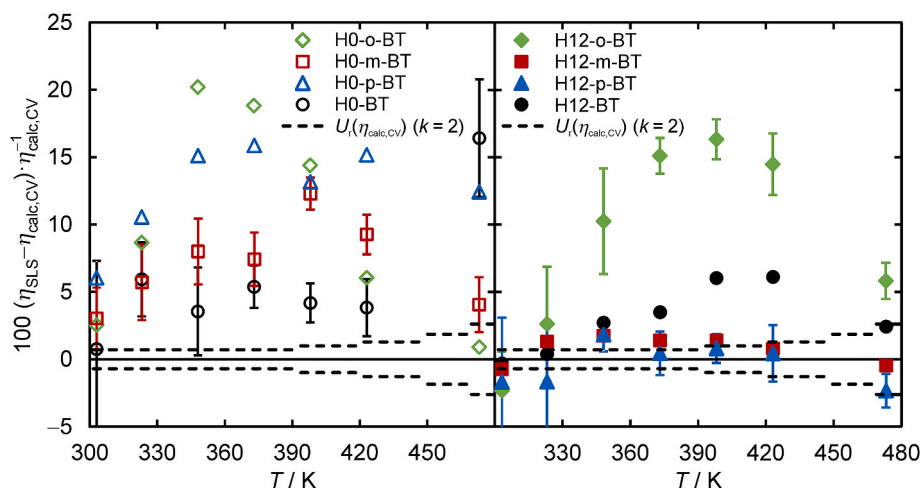


Fig. 9. Relative deviation of η values obtained by SLS for the H0-BT regioisomers and H0-BT (left) as well as the H12-BT regioisomers and H12-BT (right) from corresponding fits of the results measured by CV according to Eq. (7) as a function of T . (For interpretation of the references to color in this figure legend, the reader is referred to the Web version of this article.)

related to the effects of other surfactant-like impurities influencing the dynamics of the surface waves, which could be among the high-boilers found in the GC analysis. The observation made for η of H12-o-BT is in line with that found for σ in Fig. 4.

Considering the discussed effects observed in the SLS experiments for some samples, the following discussion especially in the context of the η behavior of mixtures will be mainly based on CV data. Nevertheless, the results for η obtained by SLS especially for the fully hydrogenated samples with the exception of H12-o-BT can be considered to be reliable and represent valuable data over an extended T range up to 573 K.

3.3.1. Pure regioisomers

Fig. 10 displays η of the H0- and H12-BT regioisomers obtained by CV as a function of T up to 473 K (upper part) and their relative deviations from η_{calc} of H0-o-BT (lower part). The data for the technical mixtures H0-BT and H12-BT are also included for a connection to mixture data discussed later on. At $T = 303$ K, η of the regioisomer samples ranges between 2.63 mPa·s for H0-p-BT and 4.68 mPa·s for both H12-o-BT and H12-p-BT. For T up to 423 K, the H12-BT regioisomers exhibit larger η values than all H0-BT regioisomers. For the individual regioisomer pairs, this statement holds up to $T = 473$ K. With increasing T , the differences in η generally become smaller, resulting in a maximum relative difference of 11%

between η of all regioisomer samples at $T = 473$ K and, considering the results from SLS, 10% at $T = 573$ K. While H0-p-BT exhibits always the smallest η values among all studied samples, the order with respect to η changes for some samples due to a different T -dependent behavior. With increasing T , η of H12-m-BT, for instance, approaches values close to those of H0-m-BT and below η of H0-o-BT for $T > 398$ K. This shows that with increasing T , it becomes more and more difficult to relate the viscosity behavior of the different isomers to specific aspects regarding molecular geometry and interactions.

In the dehydrogenated case, H0-p-BT has the lowest viscosity being by (33 and 11)% smaller than that of H0-o-BT and H0-m-BT at $T = 303$ K, where the order of these regioisomers is in accordance with that for ρ . Besides the slightly closer packing of molecules, it may be speculated that H0-o-BT also exhibits a stronger geometry-based interaction between the molecules than H0-m-BT and H0-p-BT. This might be related to the slight rotation of the methylphenyl ring plane relative to the phenyl ring plane in the case of H0-o-BT induced by the vicinity of the methyl and methylene group, which is not given for the meta- and para-isomer. For the three H0-BT isomers, the data from Lamneck and Wise [27] measured by CV and included in the lower part of Fig. 10 show very good agreement with the present CV data with deviations smaller than $\pm 0.8\%$. The structurally similar isomers of xylene, however, were reported to exhibit a different order with slightly larger η for the para-isomer than the meta-species, whereas the ortho-isomer shows the largest η of all variants [26]. From this, it may be concluded that the effects of regioisomerism on η can be different for mono- and bicyclic aromatic hydrocarbons.

In contrast to the dehydrogenated regioisomers, H12-m-BT shows the smallest η values among the hydrogenated samples. These values are by 7% smaller than those for H12-o-BT and H12-p-BT at $T = 303$ K. This order differs from that observed for ρ and is affected by the shares of *cis* and *trans* stereoisomers in the respective regioisomers studied here. To deepen the corresponding analysis, the experimental data from Lamneck and Wise [27] on the isolated conformers of the three hydrogenated regioisomers, in their work referred to as high-boiling and low-boiling isomers, are considered. For this, the directly measured kinematic viscosities ν reported in their work were converted to η values using the T -dependent density correlations ρ_{calc} obtained via Eq. (2) for the hydrogenated regioisomers, neglecting small differences in ρ of the pure stereoisomers and their mixtures studied in this work. The interpretation of the high- and low-boiling isomers as *cis* or *trans* is used analogously to the approach described in the section 3.1. Fig. 10 shows that the η values of the different stereoisomers of a given regioisomer exhibit relatively large differences of up to 34% for the ortho-isomers at $T = 311$ K. Apparently, the stereoisomeric orientation of the methyl group relative to the methylene group has a significant influence on the interactions between the molecules in the liquid phase. However, it is difficult to identify the exact reason behind this relatively strong dependence of η on the conformational orientation of the methyl group. To enable a comparison with the present results, the Arrhenius mixing rule [74] was applied to calculate η_{mix} according to $\ln(\eta_{\text{mix}}) = x_1 \ln(\eta_1) + x_2 \ln(\eta_2)$. For this, the molar compositions of the stereoisomeric mixtures studied here and the η data of the pure stereoisomers provided by Lamneck and Wise [27] were employed. Despite the simplicity of this mixing rule, good agreement between the calculated values and the CV data obtained in this work can be found for all three regioisomers. This is documented by the average relative deviations of the calculated data from the T -dependent fit of the present CV data of (−0.85, −0.25, and +0.23)% for H12-o-BT, H12-m-BT, and H12-p-BT, respectively, in the applicable T range.

Further experimental η data for the H0- and H12-BT regioisomers are only reported by Kim et al. [21], who applied rotational viscometry at T between (278 and 298) K and did not specify the stereoisomeric composition of the H12-BT regioisomer samples. At $T = 298$ K, the relative deviations of their experimental values from the extrapolated η_{calc} values based on the present CV results are +(5.6, 65, and 65)% for

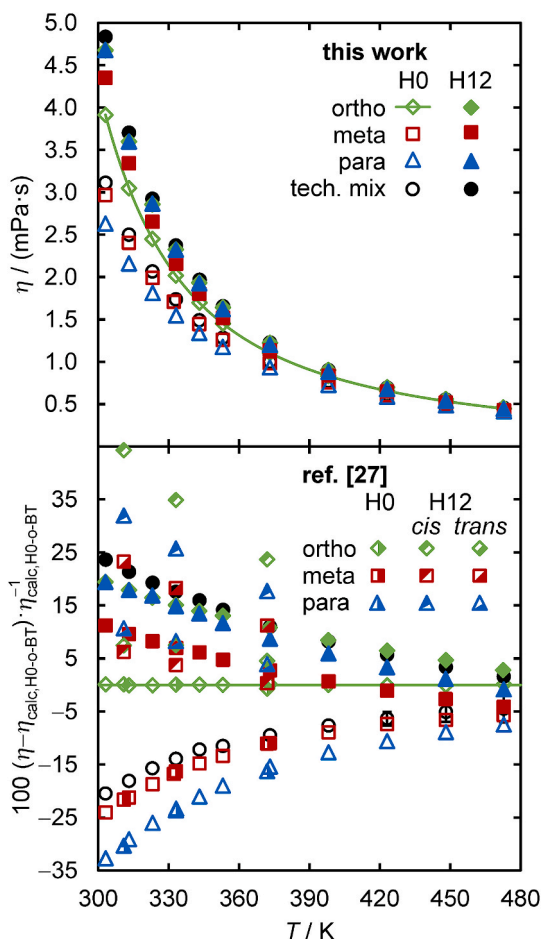


Fig. 10. Viscosity of the H0- and H12-BT regioisomers as well as of H0-BT and H12-BT obtained by CV as a function of T (upper part) and relative deviations of the data from the T -dependent fit η_{calc} of H0-o-BT according to Eq. (7) (lower part). In the lower part, experimental η values from the literature [27] for the H0-BT regioisomers as well as for the isolated *cis* and *trans* conformers of the H12-BT regioisomers are included. The interpretation of the high-boiling and low-boiling isomers of H12-BT reported by Lamneck and Wise [27] as *cis* and *trans* is described in the text. (For interpretation of the references to color in this figure legend, the reader is referred to the Web version of this article.)

H0-o-BT, H0-m-BT, and H0-p-BT, respectively, and (+9.5, −14, and −0.7)% for the corresponding hydrogenated regioisomers. It remains unclear where these large differences originate from, especially for H0-m-BT and H0-p-BT. Considering that the results from Kim et al. [21] for the commercial mixture of H0-BT show significantly lower η values than the corresponding isomers, it may be speculated that impurities present in particular in their synthesized regioisomers are responsible for this behavior.

3.3.2. Mixtures of H0-BT or H12-BT regioisomers

The behavior of η in binary and ternary regioisomer mixtures of the same *DoH* as a function of T based on the CV data is illustrated in Fig. 11 for the dehydrogenated (left) and the fully hydrogenated (right) case. On the left side of Fig. 11, H0-BT_{mix} mixed from the synthesized pure regioisomers shows slightly larger η values compared to the technical H0-BT with the same regioisomer shares, where relative deviations are up to 1.3% at $T = 303$ K. The deviations being still within combined uncertainties ($k = 2$) indicate a minor influence of the different amounts and types of impurities in these samples. The comparison of η of H0-o/p-50 with that of H0-BT_{mix} shows a nearly negligible influence of the small share of H0-m-BT, $x_{\text{H0-m-BT}} = 0.054$, in the ternary mixture. For H0-BT_{equi} with a distinctly larger share of H0-m-BT, η is by less than 1.4% smaller than that of H0-BT_{mix}. Despite the considerable variation in composition, the small variation in η is related to the relatively small difference in η of H0-m-BT and H0-BT, as evident in Fig. 10, and the almost unchanged ratio of H0-o-BT to H0-p-BT. The data for the binary mixtures H0-o/p-25 and H0-o/p-75 demonstrate, however, that considerably larger changes in η are possible for varying ratios of H0-o-BT to H0-p-BT, with relative deviations of up to −9% and +11% from H0-BT_{mix} at $T = 303$ K. As for the pure regioisomers, the differences in η of the mixtures decrease with increasing T .

For the fully hydrogenated mixtures on the right side of Fig. 11, a relatively large difference in η of H12-BT_{mix} and H12-BT is observed although both mixtures have the same regioisomeric composition. Here, besides possible influences of varying amounts and/or types of impurities, the deviations are probably mainly related to the difference in the stereoisomeric compositions of H12-BT and of the hydrogenated regioisomers used for mixing H12-BT_{mix}, cf. Table 1 and Table 2. These differences in the fractions of *cis* and *trans* conformers of a given regioisomer are presumably related to the slightly different reaction conditions applied for the synthesis of H12-BT and the three fully hydrogenated regioisomers. η of H12-o/p-50 shows on average by 0.7% larger values than H12-BT_{mix}, indicating a somewhat larger influence of the meta-isomer on η of the ternary hydrogenated mixture compared to the dehydrogenated case. Similarly, H12-BT_{equi} containing an increased share of H12-m-BT shows about 2% smaller η values than H12-BT_{mix}

since H12-m-BT exhibits by far the smallest η of the mixture compounds.

For all regioisomeric mixtures of a given *DoH*, the Arrhenius mixing rule [74] was applied to calculate η_{mix} based on the correlations η_{calc} obtained for the individual regioisomers. Here, hydrogenated samples of the regioisomers, which are mixtures of stereoisomers, are treated as pure mixture components. Considering only the mixtures prepared from the pure regioisomers, an AARD of the calculated from the experimental values of 0.75% for $T = 303$ K and 0.38% for all T was obtained. This shows that based on the presented data for the pure regioisomers and their shares in isomeric mixtures, the corresponding viscosities can be estimated rather accurately this way. A further comparison of this approach with literature data is not possible because Müller et al. [32], who measured η of isomeric mixtures of H0-BT and H12-BT, did not specify the regioisomeric compositions of their samples.

3.3.3. Mixtures of H0- and H12-ortho-BT with varying *DoH*

The *DoH*-dependent behavior of η was studied by CV for binary mixtures of H0-o-BT and H12-o-BT. The corresponding results for the mixtures as well as the pure mixture components are shown in Fig. 12 as a function of *DoH* exemplarily for $T = (303, 323, \text{ and } 353)$ K. The

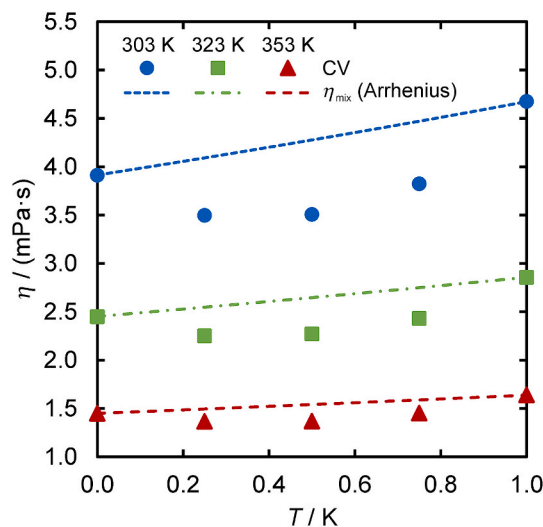


Fig. 12. Viscosity of binary mixtures of H0-o-BT and H12-o-BT as a function of *DoH* for selected T . For comparison purposes, η_{mix} obtained from the Arrhenius mixing rule [74] at corresponding T , which cannot represent the mixture behavior, is included. (For interpretation of the references to color in this figure legend, the reader is referred to the Web version of this article.)

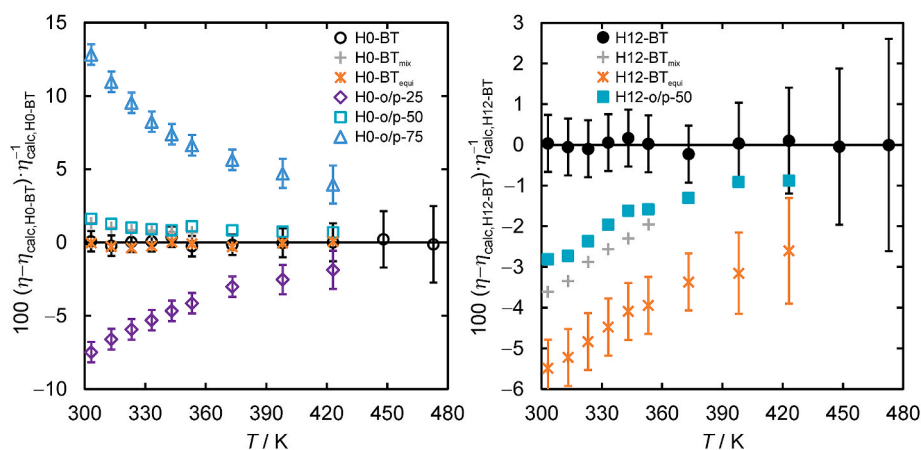


Fig. 11. Relative deviations of η of binary and ternary regioisomeric mixtures of the same *DoH* measured by CV from η_{calc} calculated according to Eq. (7) for H0-BT (left) and H12-BT (right) as a function of T . (For interpretation of the references to color in this figure legend, the reader is referred to the Web version of this article.)

mixtures exhibit a strongly nonlinear *DoH*-dependent trend with a minimum in η at a *DoH* between 0.25 and 0.50 for all T . A similar behavior with a pronounced minimum in η has also been reported for further binary mixtures of aromatic and aliphatic cyclic compounds such as benzene and cyclohexane [75], toluene and methylcyclohexane [76], and H0-DPM and H12-DPM [38]. For all these substance pairs, the η behavior is presumably related to weaker interactions between unlike molecules compared to those between alike molecules.

For the estimation of η of the mixtures of H0-o-BT and H12-o-BT, several mixing rules have been tested where H12-o-BT was treated as a pure substance. Simple approaches such as the Arrhenius mixing rule [74], cf. Fig. 12, or the Katti-Chaudri mixing rule [77] taking into account the molar volumes of the mixture components cannot describe the nonlinear *DoH*-dependent trend without any interaction parameters and result in AARDs of (13.9 or 13.3)% from the experimental values. A calculation scheme based on the extended hard-sphere model [78] was successfully applied to describe η of binary and ternary mixtures of the DPM-based LOHC system using mixing rules for the underlying model parameters as described in Ref. [38]. This model is partially capable of representing the trend of the present BT-based mixtures. However, corresponding data for η are generally slightly overestimated, resulting in an AARD of 3.8% from the experimental values when the measured ρ data are considered as input. This deviation is somewhat larger than for the DPM-based system, which may be related to the fact that the parametrization of the extended hard-sphere model for H12-o-BT consisting of two stereoisomers with significantly different η values is not sufficiently accurate. To achieve more accurate results, a model parametrization for the individual stereoisomers could be conceivable, but is currently limited due to the small amount of available η data. In summary, it is obvious that modeling the *DoH*-dependent behavior of η for the present quasi-binary system is already very challenging. Since in real processes not only the regio- and stereoisomer distributions are usually not well-known and may vary strongly, but also various H6-BT isomers can have further significant impacts, no specific approaches of representing the mixture viscosity at varying *DoH* based on the values for the mixture components are recommended here.

3.3.4. H12-o-BT in the presence of pressurized H₂

The experimental results for η of H12-o-BT under the influence of pressurized H₂ at $T = (323, 423, \text{ and } 523) \text{ K}$ obtained from SLS are presented in Fig. 13 in terms of their relative deviations from the

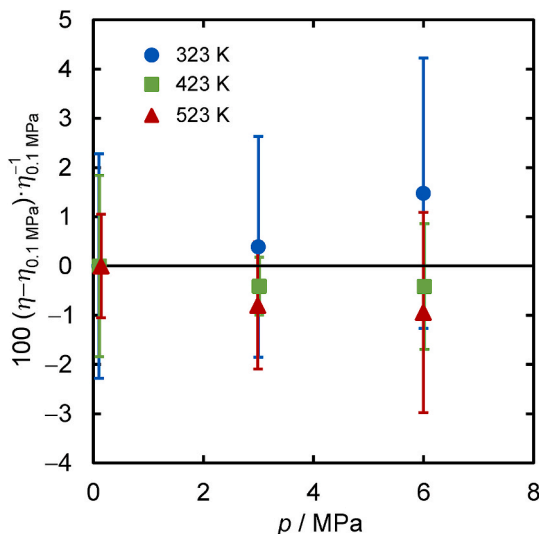


Fig. 13. Relative deviations of η of H12-o-BT in the presence of a H₂ atmosphere from the values at $p \approx 0.1 \text{ MPa}$ as a function of p measured by SLS. (For interpretation of the references to color in this figure legend, the reader is referred to the Web version of this article.)

reference value at the same T measured under H₂ atmosphere at $p \approx 0.1 \text{ MPa}$, $\eta_{0.1 \text{ MPa}}$, as a function of p . As discussed before in connection with σ in Fig. 8, the anticipated presence of impurities in the H12-o-BT sample introducing viscoelastic effects leads to not fully reliable absolute η values for H12-o-BT saturated with H₂ determined by SLS. Nevertheless, these values may allow for a relative comparison between the apparent results at different p at a given T . All relative deviations of η measured up to $p = 6 \text{ MPa}$ from the respective reference values obtained at $p \approx 0.1 \text{ MPa}$ are within the experimental uncertainty ($k = 2$) of the latter and always smaller than $\pm 1.5\%$. This indicates a rather p -independent behavior of η as a function of p for H12-o-BT in the presence of pressurized H₂, from which also an x_{H_2} -independent behavior can be inferred for vapor-liquid equilibrium conditions. A p -independent behavior of η has also been observed for the structurally similar H12-DPM saturated with pressurized H₂ at p up to 7 MPa and in the same T range as in the present study [34]. For this previously studied system, viscoelastic effects originating from impurities can be excluded with great certainty. Thus, the agreeing trends for the H12-DPM-based system with that for the present H12-o-BT-based system indicate that the relative comparison of the results in this work gives an accurate picture of the p -dependent behavior of η of H12-o-BT saturated with H₂ despite the likely presence of viscoelastic effects. While for pure fluids, η typically increases with increasing p in the compressed liquid phase [79], it appears that the dissolved H₂ has a counterbalancing effect of similar magnitude which results in the nearly p -independent behavior. This trend goes along with the widely p - and x_{H_2} -independent behavior of ρ of H12-o-BT saturated with pressurized H₂ reported in Ref. [53], which was considered for the evaluation of the present SLS data. Since the same behavior of η was observed for H0-DPM as well as its mixtures with H12-DPM at varying *DoH* saturated with H₂ [34], a rather p -independent behavior of η in the presence of H₂ can also be expected for other BT-based samples independent of the *DoH*. The influence of dissolved H₂ on η of further organic fluids in or close to vapor-liquid equilibrium was addressed in only a few studies in the literature. For *n*-hexadecane [69], *n*-octacosane [73], benzene [80], cyclohexane [80], and methanol [70], a mostly p -independent behavior is reported. For *n*-pentane, Al-Harbi et al. [80] found an increase in η by up to 4% with an increase in p by 2.7 MPa, while for 1-hexadecanol [73] and a crude oil [81], a decrease of about 5% in η was measured upon an increase in p by (7.0 and 3.4) MPa, respectively.

3.4. Thermal and Fick diffusivities

The values for the thermal diffusivity α and Fick diffusion coefficient D_{11} of H12-o-BT with dissolved H₂ at $p = 6.0 \text{ MPa}$ and T between (323 and 523) K determined from DLS experiments are listed in Table S13 in the Supporting Information together with the corresponding relative uncertainties ($k = 2$), which are on average $U_r(\alpha) = 9.7\%$ and $U_r(D_{11}) = 22\%$. The relatively small values for x_{H_2} , which were determined based on solubility data from Ref. [53], range from 0.041 to 0.086 and indicate that conditions close to infinite dilution can be assumed. Furthermore, the studied H₂-LOHC mixtures can be treated as pseudo-binary mixtures since the *cis* and *trans* stereoisomers of H12-o-BT are expected to be indistinguishable in the DLS signal related to concentration fluctuations. For $T = (473 \text{ and } 523) \text{ K}$, the two exponentially decaying modes in the recorded intensity CFs associated with fluctuations in temperature and concentration and giving simultaneous access to α and D_{11} were relatively similar with respect to their signal amplitudes and characteristic decay times and, consequently, could not be separated. As a result, only a mixed diffusivity D_{mix} could be obtained which cannot be associated purely with either α or D_{11} . Corresponding uncertainties for D_{mix} cannot be quantified reliably and are, thus, not shown.

The obtained results for α , D_{11} , and D_{mix} are depicted as a function of T in Fig. 14. α decreases by 30% with increasing T from (323 to 423) K. Typically, the influence of the dissolved gas for the given x_{H_2} range on α

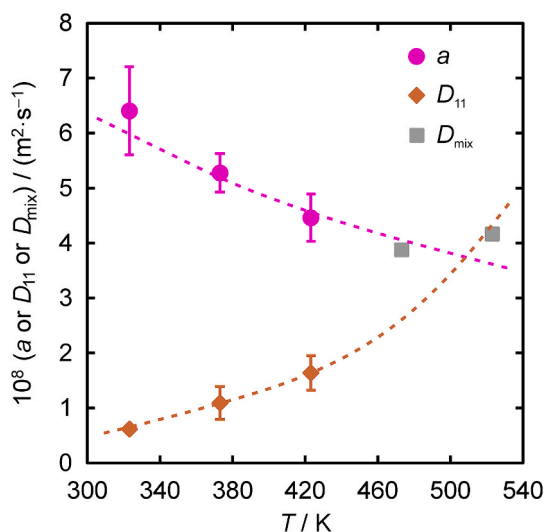


Fig. 14. Thermal and Fick diffusivities a and D_{11} as well as mixed diffusivities D_{mix} of H12-o-BT containing dissolved H_2 at $p = 6.0$ MPa close to infinite dilution of H_2 as a function of T . The lines indicating the T -dependent trend of a and D_{11} serve as a guide for the eye. (For interpretation of the references to color in this figure legend, the reader is referred to the Web version of this article.)

of the solvent is small compared to the experimental uncertainties [82, 83] and, thus, the measured a values can be assumed to be close to those for pure H12-o-BT. No data for a of pure H12-o-BT or its mixture with H_2 could be found in the literature. D_{11} obtained by DLS increases strongly by a factor of about 2.7 from $(6.2\text{--}16) \cdot 10^{-9} \text{ m}^2 \text{ s}^{-1}$ at $T = (323\text{--}423)$ K. To the best of our knowledge, no corresponding data for H12-o-BT containing dissolved H_2 are reported in the literature. In the case of the structurally similar H12-DPM, D_{11} values reported for its mixture with dissolved H_2 [84] are in the given T range by (23–49)% larger. For $T = (473 \text{ and } 523)$ K, a detailed discussion of the D_{mix} values would be rather speculative and is therefore not included here.

4. Conclusions

The present work comprises an extensive experimental study on the density ρ , surface or interfacial tension σ , and dynamic viscosity η of pure H0- and H12-BT regioisomers specifically synthesized for these investigations and of BT-based mixtures at T ranging from (283 to 573) K close to ambient p . In addition, the influence of pressurized H_2 on σ and η was studied exemplarily for the regioisomer H12-o-BT at T up to 523 K and p up to 6 MPa, where also thermal diffusivities a and Fick diffusion coefficients D_{11} could be determined. The present experimental data obtained from several measurement methods extend the current data situation in the literature for this LOHC system considerably and helps to approximate the properties of commercial BT products via determination of their isomeric composition.

While ρ of the H12-BT regioisomers is up to about 13% smaller than that of corresponding H0-BT samples, comparably small differences in ρ among the H0- or H12-BT regioisomers of less than 1.6% were found. ρ of the H0-BT or H12-BT regioisomer mixtures can be described well by a molar-volume-based mixing rule with an AARD of 0.022% of the calculated from the experimental data. For binary mixtures of H0-o-BT and H12-o-BT, an excess molar volume of up to $+0.6 \text{ cm}^3 \text{ mol}^{-1}$ was found. σ of the H12-BT regioisomers is up to (18 and 24)% smaller than the corresponding H0-BT species at $T = (303 \text{ and } 523)$ K, whereas relatively small differences within 4% were found between the samples at a given DoH . The nonlinear DoH -dependent behavior of σ in binary mixtures of H0-o-BT and H12-o-BT could be modeled using the

empirical approach proposed by Vakili-Nezhaad [66,67] with an AARD of 2.0% from the measured results. η of the H12-BT regioisomers is generally larger than that of their dehydrogenated counterparts. Here, the corresponding relative differences decrease strongly with increasing T from up to 78% at $T = 303$ K to below 7.2% at $T = 473$ K. Among the H0-BT or H12-BT regioisomers, η varies by up to 33% at the lowest T , which leads to a significant dependence of η on the actual isomeric mixture composition that can be relevant for technical processes. For the dehydrogenated or fully hydrogenated regioisomer mixtures, the simple Arrhenius mixing rule [74] can describe the measured values up to $T = 473$ K well with an AARD of 0.38%. The DoH -dependent behavior of η in binary mixtures of H0-o-BT and H12-o-BT exhibits a pronounced minimum, which cannot be captured by simple estimation schemes. For H12-o-BT in the presence of pressurized H_2 , σ , η , a , and D_{11} were studied by means of the PD method, SLS, and DLS at T up to 523 K and p up to 6 MPa. The results show a slight decrease of σ with increasing p by up to 5% at 6 MPa and a mostly p -independent behavior of η for all T , which corresponds to reported findings for the DPM-based LOHC system [34]. a and D_{11} for H12-o-BT containing dissolved H_2 at conditions close to infinite dilution show a decreasing and increasing trend, respectively, with increasing T .

Funding sources

This work was funded by the Bavarian Ministry of Economic Affairs, Regional Development and Energy as well as by the German Research Foundation (Deutsche Forschungsgemeinschaft, DFG) under Grant No. FR 1709/27-1.

CRediT authorship contribution statement

Manuel Kerscher: Writing – original draft, Methodology, Investigation, Formal analysis. **Julius H. Jander:** Writing – review & editing, Methodology, Investigation, Formal analysis. **Junwei Cui:** Investigation, Formal analysis. **Lukas A. Maurer:** Resources. **Patrick Wolf:** Resources. **Jonas D. Hofmann:** Resources. **Anil Köksal:** Investigation, Formal analysis. **Hannah Zachskorn:** Investigation, Formal analysis. **Franziska Auer:** Resources. **Peter S. Schulz:** Writing – review & editing, Investigation, Formal analysis. **Peter Wasserscheid:** Writing – review & editing, Resources, Conceptualization. **Michael H. Rausch:** Writing – review & editing, Supervision, Project administration, Investigation, Conceptualization. **Thomas M. Koller:** Writing – review & editing, Supervision, Project administration. **Andreas P. Fröba:** Writing – review & editing, Supervision, Resources, Project administration, Conceptualization.

Declaration of competing interest

The authors declare that they have no known competing financial interests or personal relationships that could have appeared to influence the work reported in this paper.

Acknowledgements

The authors gratefully acknowledge funding of the Erlangen Graduate School in Advanced Optical Technologies by the Bavarian State Ministry for Science and Art.

Appendix A. Supplementary data

Supplementary data to this article can be found online at <https://doi.org/10.1016/j.ijhydene.2024.06.131>.

References

- [1] Durbin DJ, Malardier-Jugroot C. Review of hydrogen storage techniques for on board vehicle applications. *Int J Hydrogen Energy* 2013;38:14595–617. <https://doi.org/10.1016/j.ijhydene.2013.07.058>.
- [2] Faye O, Szpunar J, Eduok U. A critical review on the current technologies for the generation, storage, and transportation of hydrogen. *Int J Hydrogen Energy* 2022;47:13771–802. <https://doi.org/10.1016/j.ijhydene.2022.02.112>.
- [3] Samantary SS, Putnam ST, Stadie NP. Volumetrics of hydrogen storage by physical adsorption. *Inorganics* 2021;9:45. <https://doi.org/10.3390/inorganics9060045>.
- [4] Mananghaya MR. Titanium-decorated boron nitride nanotubes for hydrogen storage: a multiscale theoretical investigation. *Nanoscale* 2019;11:16052–62. <https://doi.org/10.1039/C9NR04578C>.
- [5] Stetson N, Wieliczko M. Hydrogen technologies for energy storage: a perspective. *MRS Energy Sustain* 2020;7:1–9. <https://doi.org/10.1557/mre.2020.43>.
- [6] Tarasov BP, Fursikov PV, Volodin AA, Bocharnikov MS, Shimkus YY, Kashin AM, Yartys VA, Chidziva S, Pasupathi S, Lototsky MV. Metal hydride hydrogen storage and compression systems for energy storage technologies. *Int J Hydrogen Energy* 2021;46:13647–57. <https://doi.org/10.1016/j.ijhydene.2020.07.085>.
- [7] Moioili E, Schildhauer T. Eco-techno-economic analysis of methanol production from biogas and power-to-X. *Ind Eng Chem Res* 2022;61:7335–48. <https://doi.org/10.1021/acs.iecr.1c04682>.
- [8] García G, Arriola E, Chen W-H, De Luna MD. A comprehensive review of hydrogen production from methanol thermochemical conversion for sustainability. *Energy* 2021;217:119384. <https://doi.org/10.1016/j.energy.2020.119384>.
- [9] Preuster P, Alekseev A, Wasserscheid P. Hydrogen storage technologies for future energy systems. *Annu Rev Chem Biomol Eng* 2017;8:445–71. <https://doi.org/10.1146/annurev-chembioeng-060816-101334>.
- [10] Andersson J, Grönkvist S. Large-scale storage of hydrogen. *Int J Hydrogen Energy* 2019;44:11901–19. <https://doi.org/10.1016/j.ijhydene.2019.03.063>.
- [11] Perreault P, Van Hoecke L, Pourfallah H, Kummamuru NB, Borutnea C-R, Preuster P. Critical challenges towards the commercial rollouts of a LOHC-based H₂ economy. *Curr Opin Green Sustainable Chem* 2023;41:100836. <https://doi.org/10.1016/j.cogsc.2023.100836>.
- [12] Rao P, Yoon M. Potential liquid-organic hydrogen carrier (LOHC) systems: a review on recent progress. *Energies* 2020;13:6040. <https://doi.org/10.3390/en13226040>.
- [13] Makepeace JW, He T, Weidenthaler C, Jensen TR, Chang F, Vegge T, Ngene P, Kojima Y, de Jongh PE, Chen P, David WIF. Reversible ammonia-based and liquid organic hydrogen carriers for high-density hydrogen storage: recent progress. *Int J Hydrogen Energy* 2019;44:7746–67. <https://doi.org/10.1016/j.ijhydene.2019.01.144>.
- [14] Niermann M, Beckendorff A, Kaltschmitt M, Bonhoff K. Liquid organic hydrogen carrier (LOHC) – assessment based on chemical and economic properties. *Int J Hydrogen Energy* 2019;44:6631–54. <https://doi.org/10.1016/j.ijhydene.2019.01.199>.
- [15] Niermann M, Timmerberg S, Drüner S, Kaltschmitt M. Liquid organic hydrogen carriers and alternatives for international transport of renewable hydrogen. *Renew Sustain Energy Rev* 2021;135:110171. <https://doi.org/10.1016/j.rser.2020.110171>.
- [16] Stark K, Keil P, Schug S, Müller K, Wasserscheid P, Arlt W. Melting points of potential liquid organic hydrogen carrier systems consisting of N-alkylcarbazoles. *J Chem Eng Data* 2016;61:1441–8. <https://doi.org/10.1021/acs.jced.5b00679>.
- [17] Crabtree RH. Nitrogen-containing liquid organic hydrogen carriers: progress and prospects. *ACS Sustainable Chem Eng* 2017;5:4491–8. <https://doi.org/10.1021/acssuschemeng.7b00983>.
- [18] Spatolisano E, Matichicchia A, Pellegrini LA, de Angelis AR, Cattaneo S, Roccaro E. Toluene as effective LOHC: detailed techno-economic assessment to identify challenges and opportunities. In: Kokossis AC, Georgiadis MC, Pistikopoulos E, editors. 33rd Eur. Symp. Comput. Aided process eng., 52. Elsevier; 2023. p. 3245–50. <https://doi.org/10.1016/B978-0-443-15274-0.50517-5>.
- [19] Jorschick H, Geißelbrecht M, Ebl M, Preuster P, Bösmann A, Wasserscheid P. Benzyltoluene/dibenzyltoluene-based mixtures as suitable liquid organic hydrogen carrier systems for low temperature applications. *Int J Hydrogen Energy* 2020;45:14897–906. <https://doi.org/10.1016/j.ijhydene.2020.03.210>.
- [20] Rüde T, Lu Y, Anschutz L, Blasius M, Wolf M, Preuster P, Wasserscheid P, Geißelbrecht M. Performance of continuous hydrogen production from perhydro benzyltoluene by catalytic distillation and heat integration concepts with a fuel cell. *Energy Technol* 2023;2201366. <https://doi.org/10.1002/ente.202201366>.
- [21] Kim TW, Jo Y, Jeong K, Yook H, Han JW, Jang JH, Han GB, Park JH, Suh Y-W. Tuning the isomer composition is a key to overcome the performance limits of commercial benzyltoluene as liquid organic hydrogen carrier. *J Energy Storage* 2023;60:106676. <https://doi.org/10.1016/j.est.2023.106676>.
- [22] Preuster P, Papp C, Wasserscheid P. Liquid organic hydrogen carriers (LOHCs): toward a hydrogen-free hydrogen economy. *Acc Chem Res* 2017;50:74–85. <https://doi.org/10.1021/acs.accounts.6b00474>.
- [23] Rüde T, Dürr S, Preuster P, Wolf M, Wasserscheid P. Benzyltoluene/perhydro benzyltoluene – pushing the performance limits of pure hydrocarbon liquid organic hydrogen carrier (LOHC) systems. *Sustain Energy Fuels* 2022;6:1541–53. <https://doi.org/10.1039/D1SE01767E>.
- [24] Kwak Y, Kirk J, Moon S, Ohm T, Lee Y-J, Jang M, Park L-H, Ahn C, Jeong H, Sohn H, Nam SW, Yoon CW, Jo YS, Kim Y. Hydrogen production from homocyclic liquid organic hydrogen carriers (LOHCs): benchmarking studies and energy-economic analyses. *Energy Convers Manag* 2021;239:114124. <https://doi.org/10.1016/j.enconman.2021.114124>.
- [25] Leinweber A, Müller K. Hydrogenation of the liquid organic hydrogen carrier compound monobenzyl toluene: reaction pathway and kinetic effects. *Energy Technol* 2018;6:513–20. <https://doi.org/10.1002/ente.201700376>.
- [26] Al-Kandary JA, Al-Jimaz AS, Abdul-Latif AHM. Viscosities, densities, and speeds of sound of binary mixtures of benzene, toluene, o-xylene, m-xylene, p-xylene, and mesitylene with anisole at (288.15, 293.15, 298.15, and 303.15) K. *J Chem Eng Data* 2006;51:2074–82. <https://doi.org/10.1021/jc060170c>.
- [27] Lamneck JH, Wise PH. Dicyclic hydrocarbons. IX. Synthesis and physical properties of the monomethyldiphenylmethanes and monomethyldicyclohexylmethanes. *J Am Chem Soc* 1954;76:1104–6. <https://doi.org/10.1021/ja01633a050>.
- [28] Senff P. Ueber Meta-Benzyltoluol, Meta-Tolylphenylketon, Meta-Benzoylbenzoesäure und deren Reduktionsprodukte. *Liebigs Ann* 1883;220:225–53. <https://doi.org/10.1002/jlac.18832200302>.
- [29] Klages A, Allendorff P. Ueber die Reduction aromatischer Ketone durch Natrium und Alkohol. *Ber Dtsch Chem Ges* 1898;31:998–1010. <https://doi.org/10.1002/cber.189803101182>.
- [30] Good WD, Lee SH. The enthalpies of formation of selected naphthalenes, diphenylmethanes, and bicyclic hydrocarbons. *J Chem Thermodyn* 1976;8:643–50. [https://doi.org/10.1016/0021-9614\(76\)90015-X](https://doi.org/10.1016/0021-9614(76)90015-X).
- [31] Hennion GF, Kurtz RA. Some Friedel-Crafts type alkylations with boron trifluoride. *J Am Chem Soc* 1943;65:1001–3. <https://doi.org/10.1021/ja01246a002>.
- [32] Müller K, Stark K, Emel'yanenko VN, Varfolomeev MA, Zaitsau DH, Shofet E, Schick C, Verevkin SP, Arlt W. Liquid organic hydrogen carriers: thermophysical and thermochemical studies of benzyl- and dibenzyl-toluene derivatives. *Ind Eng Chem Res* 2015;54:7967–76. <https://doi.org/10.1021/acs.iecr.5b01840>.
- [33] Jander JH, Schmidt PS, Giraudet C, Wasserscheid P, Rausch MH, Fröba AP. Hydrogen solubility, interfacial tension, and density of the liquid organic hydrogen carrier system diphenylmethane/dicyclohexylmethane. *Int J Hydrogen Energy* 2021;46:19446–66. <https://doi.org/10.1016/j.ijhydene.2021.03.093>.
- [34] Kerscher M, Klein T, Preuster P, Wasserscheid P, Koller TM, Rausch MH, Fröba AP. Influence of dissolved hydrogen on the viscosity and interfacial tension of the liquid organic hydrogen carrier system based on diphenylmethane by surface light scattering and molecular dynamics simulations. *Int J Hydrogen Energy* 2022;47:39163–78. <https://doi.org/10.1016/j.ijhydene.2022.09.078>.
- [35] Kerscher M, Jander JH, Cui J, Martin MM, Wolf M, Preuster P, Rausch MH, Wasserscheid P, Koller TM, Fröba AP. Viscosity, surface tension, and density of binary mixtures of the liquid organic hydrogen carrier diphenylmethane with benzophenone. *Int J Hydrogen Energy* 2022;47:15789–806. <https://doi.org/10.1016/j.ijhydene.2022.03.051>.
- [36] Shi L, Qi S, Qu J, Che T, Yi C, Yang B. Integration of hydrogenation and dehydrogenation based on dibenzyltoluene as liquid organic hydrogen energy carrier. *Int J Hydrogen Energy* 2019;5345–54. <https://doi.org/10.1016/j.ijhydene.2018.09.083>.
- [37] Cho J-Y, Kim H, Oh J-E, Park BY. Recent advances in homogeneous/heterogeneous catalytic hydrogenation and dehydrogenation for potential liquid organic hydrogen carrier (LOHC) systems. *Catalysts* 2021;11:1497. <https://doi.org/10.3390/catal11121497>.
- [38] SDBSWeb (National Institute of Advanced Industrial Science and Technology). <https://sdb.sdb.aist.go.jp> (accessed July 7, 2023).
- [39] Schmidt PS, Kerscher M, Klein T, Jander JH, Berger Bioucas FE, Rüde T, Li S, Stadelmaier M, Hanyon S, Fathalla RR, Bösmann A, Preuster P, Wasserscheid P, Koller TM, Rausch MH, Fröba AP. Effect of the degree of hydrogenation on the viscosity, surface tension, and density of the liquid organic hydrogen carrier system based on diphenylmethane. *Int J Hydrogen Energy* 2022;47:6111–30. <https://doi.org/10.1016/j.ijhydene.2021.11.198>.
- [40] Rotenberg Y, Boruvka L, Neumann AW. Determination of surface tension and contact angle from the shapes of axisymmetric fluid interfaces without use of apex coordinates. *J Colloid Interface Sci* 1983;93:169–83. <https://doi.org/10.1021/la061928t>.
- [41] Hoorfar MW, Neumann A. Recent progress in axisymmetric drop shape analysis (ADSA). *Adv Colloid Interface Sci* 2006;121:25–49. <https://doi.org/10.1016/j.cis.2006.06.001>.
- [42] Saad SMI, Neumann AW. Axisymmetric drop shape analysis (ADSA): an outline. *Adv Colloid Interface Sci* 2016;238:62–87. <https://doi.org/10.1016/j.cis.2016.11.001>.
- [43] Rusanov AI, Prokhorov VA. *Interfacial tensiometry, vol. 3*. Amsterdam, New York: Elsevier; 1996.
- [44] Cui J, Kerscher M, Jander JH, Rüde T, Schulz PS, Wasserscheid P, Rausch MH, Koller TM, Fröba AP. Viscosity and surface tension of fluorene and perhydrofluorene close to 0.1 MPa up to 573 K. *J Chem Eng Data* 2022;67:3085–96. <https://doi.org/10.1021/acs.jced.2c00519>.
- [45] Kerscher M, Jander JH, Cui J, Wasserscheid P, Rausch MH, Koller TM, Fröba AP. Thermophysical properties of the liquid organic hydrogen carrier system based on diphenylmethane with the byproducts fluorene or perhydrofluorene. *Int J Hydrogen Energy* 2023;48:29651–62. <https://doi.org/10.1016/j.ijhydene.2023.04.103>.
- [46] Lucasen-Reynders EH, Lucassen J. Properties of capillary waves. *Adv Colloid Interface Sci* 1970;2:347–95. [https://doi.org/10.1016/0001-8686\(70\)80001-X](https://doi.org/10.1016/0001-8686(70)80001-X).
- [47] Langevin D. *Light scattering by liquid surfaces and complementary techniques*. New York: Dekker, Marcel; 1992.
- [48] Fröba AP, Leipertz A. Accurate determination of liquid viscosity and surface tension using surface light scattering (SLS): toluene under saturation conditions between 260 and 380 K. *Int J Thermophys* 2003;24:895–921. <https://doi.org/10.1023/A:1025097311041>.
- [49] Fröba AP, Will S. Light scattering by surface waves - surface light scattering. In: Goodwin ARH, Vesovic V, Wakeham WA, editors. *Experimental Thermodynamics*,

- Vol. IX: Advances in Transport Properties of Fluids, Assael M.J. Royal Society of Chemistry:Cambridge, U.K; 2014. p. 22–35. <https://doi.org/10.1039/9781782625254-00019>.
- [50] Ohmura Y, Hoshino T, Osada R, Yao M. Bulk shear-mode contribution to thermally generated capillary waves on a room-temperature ionic-liquid surface. *Phys Rev E - Stat Nonlinear Soft Matter Phys* 2009;79:1–11. <https://doi.org/10.1103/PhysRevE.79.061601>.
- [51] Koller TM, Kerscher M, Fröba AP. Accurate determination of viscosity and surface tension by surface light scattering in the presence of a contribution from the rotational flow in the bulk of the fluid. *J Colloid Interface Sci* 2022;626:899–915. <https://doi.org/10.1016/j.jcis.2022.06.129>.
- [52] Koller TM, Klein T, Giraudet C, Chen J, Kalantar A, van der Laan GP, Rausch MH, Fröba AP. Liquid viscosity and surface tension of *n*-dodecane, *n*-octacosane, their mixtures, and a wax between 323 and 573 K by surface light scattering. *J Chem Eng Data* 2017;62:3319–33. <https://doi.org/10.1021/acs.jced.7b00363>.
- [53] Jander JH, Kumar Chittam P, Kerscher M, Rausch MH, Wasserscheid P, Fröba AP. Raman spectroscopy for the determination of hydrogen concentration in liquid organic hydrogen carrier systems. *Int J Hydrogen Energy* 2024;73:681–94. <https://doi.org/10.1016/j.ijhydene.2024.05.381>.
- [54] Berne BJ, Pecora R. *Dynamic light scattering*. New York: Dover edit; 2000.
- [55] Will S, Leipertz A. *Thermophysical properties of fluids from dynamic light scattering*. *Int J Thermophys* 2001;22:317–38.
- [56] Fröba AP. *Dynamic light scattering (DLS) for the characterization of working fluids in chemical and energy engineering*. Habilitation thesis. Friedrich-Alexander-Universität Erlangen-Nürnberg; 2009.
- [57] Aslam R, Khan MH, Ishaq M, Müller K. Thermophysical studies of dibenzyltoluene and its partially and fully hydrogenated derivatives. *J Chem Eng Data* 2018;63: 4580–7. <https://doi.org/10.1021/acs.jced.8b00652>.
- [58] Qin A, Hoffman DE, Munk P. Excess volumes of mixtures of alkanes with carbonyl compounds. *J Chem Eng Data* 1992;37:55–61. <https://doi.org/10.1021/jc00005a018>.
- [59] Kumaran MK, Benson GC. Excess molar volumes of (benzene + cyclohexane) at 323.15 K. *J Chem Thermodyn* 1984;16:183–7. [https://doi.org/10.1016/0021-9614\(84\)90153-8](https://doi.org/10.1016/0021-9614(84)90153-8).
- [60] Peña MP, Martínez-Soria V, Montón J. Densities, refractive indices, and derived excess properties of the binary systems tert-butyl alcohol+toluene, + methylcyclohexane, and +isooctane and toluene+methylcyclohexane, and the ternary system tert-butyl alcohol+toluene+methylcyclohexane at 298.15 K. *Fluid Phase Equil* 1999;166:53–65. [https://doi.org/10.1016/S0378-3812\(99\)00284-8](https://doi.org/10.1016/S0378-3812(99)00284-8).
- [61] Earnshaw JC, McCoo E. Surface light-scattering studies of surfactant solutions. *Langmuir* 1995;11:1087–100. <https://doi.org/10.1021/la00004a011>.
- [62] Monroy F, Muñoz MG, Rubio JEF, Ortega F, Rubio RG. Capillary waves in ionic surfactant solutions: effects of the electrostatic adsorption barrier and analysis in terms of a new dispersion equation. *J Phys Chem B* 2002;106:5636–44. <https://doi.org/10.1021/jp012044f>.
- [63] Langevin D. Light scattering by liquid surfaces, new developments. *Adv Colloid Interface Sci* 2021;289:102368. <https://doi.org/10.1016/j.cis.2021.102368>.
- [64] Koller TM, Kerscher M, Köksal A, Stockerl MR, Klein T, Fröba AP. Revealing the effects of weak surfactants on the dynamics of surface fluctuations by surface light scattering. *J Phys Chem B* 2023;127:10647–58. <https://doi.org/10.1021/acs.jpcc.3c06309>.
- [65] Ouyang G, Huang Z, Ou J, Wu W, Kang B. Excess molar volumes and surface tensions of xylene with 2-propanol or 2-methyl-2-propanol at 298.15 K. *J Chem Eng Data* 2003;48:195–7. <https://doi.org/10.1021/jc0256028>.
- [66] Vakili-Nezhaad GR, Al-Wadhahi M, Al-Haddabi S, Vakilinejad A, Acree WE. Surface tension of multicomponent organic mixtures: measurement and correlation. *J Mol Liq* 2019;296:112008. <https://doi.org/10.1016/j.molliq.2019.112008>.
- [67] Vakili-Nezhaad GR, Al-Wadhahi M, Al-Haddabi S, Vakilinejad A, Acree WE. Surface tension of binary organic mixtures based on a new dimensionless number. *J Chem Thermodyn* 2021;152:106292. <https://doi.org/10.1016/j.jct.2020.106292>.
- [68] Goldsack DE, Sarvas CD. Volume fraction statistics and the surface tensions of non-electrolyte solutions. *Can J Chem* 1981;59:2968–80. <https://doi.org/10.1139/v81-431>.
- [69] Klein T, Lenahan FD, Kerscher M, Jander JH, Rausch MH, Koller TM, Fröba AP. Viscosity and interfacial tension of binary mixtures of *n*-hexadecane with dissolved gases using surface light scattering and equilibrium molecular dynamics simulations. *J Chem Eng Data* 2021;66:3205–18. <https://doi.org/10.1021/acs.jced.1c00289>.
- [70] Kerscher M, Jander JH, Luther F, Schühle P, Richter M, Rausch MH, Fröba AP. Thermophysical properties of the energy carrier methanol under the influence of dissolved hydrogen. *Int J Hydrogen Energy* 2023;48:26817–39. <https://doi.org/10.1016/j.ijhydene.2023.03.312>.
- [71] Rice OK. The effect of pressure on surface tension. *J Chem Phys* 1947;15:333–5. <https://doi.org/10.1063/1.1746507>.
- [72] Slowinski EJ, Gates EE, Waring CE. The effect of pressure on the surface tensions of liquids. *J Phys Chem* 1957;61:808–10. <https://doi.org/10.1021/j150552a028>.
- [73] Klein T, Lenahan FD, Zhai Z, Kerscher M, Jander JH, Koller TM, Rausch MH, Fröba AP. Viscosity and interfacial tension of binary mixtures consisting of linear, branched, cyclic, or oxygenated hydrocarbons with dissolved gases using surface light scattering and equilibrium molecular dynamics simulations. *Int J Thermophys* 2022;43:88. <https://doi.org/10.1007/s10765-022-03012-1>.
- [74] Arrhenius S. Über die Dissociation der in Wasser gelösten Stoffe. *Z Phys Chem* 1887;1U:631–48. <https://doi.org/10.1515/zpch-1887-0164>.
- [75] Papaioannou D, Panayiotou C, Evangelou T. Dynamic viscosity of multicomponent liquid mixtures. *J Chem Eng Data* 1991;36:43–6. <https://doi.org/10.1021/jc00001a013>.
- [76] Baragi JG, Aralaguppi MI. Excess and deviation properties for the binary mixtures of methylcyclohexane with benzene, toluene, p-xylene, mesitylene, and anisole at T = (298.15, 303.15, and 308.15) K. *J Chem Thermodyn* 2006;38:1717–24. <https://doi.org/10.1016/j.jct.2005.12.005>.
- [77] Katti PK, Chaudhri MM. Viscosities of binary mixtures of benzyl acetate with dioxane, aniline, and m-cresol. *J Chem Eng Data* 1964;9:442–3. <https://doi.org/10.1021/jc00022a047>.
- [78] Ciotta F, Trusler JPM, Vesovic V. Extended hard-sphere model for the viscosity of dense fluids. *Fluid Phase Equil* 2014;363:239–47. <https://doi.org/10.1016/j.fluid.2013.11.032>.
- [79] Lucas K. Die Druckabhängigkeit der Viskosität von Flüssigkeiten – eine einfache Abschätzung. *Chem Ing Tech* 1981;53:959–60. <https://doi.org/10.1002/cite.330531209>.
- [80] Al-Harbi DK, Maddox RN. Viscosity of hydrocarbon liquids saturated with gas. *Eng J Qatar Univ* 1995;8:31–42.
- [81] Beecher CE, Parkhurst IP. Effect of dissolved gas upon the viscosity and surface tension of crude oil. *Trans AIME* 1926;G-26:51–69. <https://doi.org/10.2118/926051-G>.
- [82] Piszko M, Lenahan FD, Hahn S, Rausch MH, Koller TM, Klein T, Fröba AP. Diffusivities in binary mixtures of *n*-hexane or 1-hexanol with dissolved CH₄, Ne, Kr, R143a, SF₆, or R236fa close to infinite dilution. *J Chem Eng Data* 2021;66: 2218–32. <https://doi.org/10.1021/acs.jced.1c00084>.
- [83] Wu W, Klein T, Kerscher M, Rausch MH, Koller TM, Giraudet C, Fröba AP. Diffusivities in 1-alcohols containing dissolved H₂, He, N₂, CO, or CO₂ close to infinite dilution. *J Phys Chem B* 2019;123:8777–90. <https://doi.org/10.1021/acs.jpcc.9b06211>.
- [84] Berger Bioucas FE, Piszko M, Kerscher M, Preuster P, Rausch MH, Koller TM, Wasserscheid P, Fröba AP. Thermal conductivity of hydrocarbon liquid organic hydrogen carrier systems: measurement and prediction. *J Chem Eng Data* 2020;65: 5003–17. <https://doi.org/10.1021/acs.jced.0c00613>.